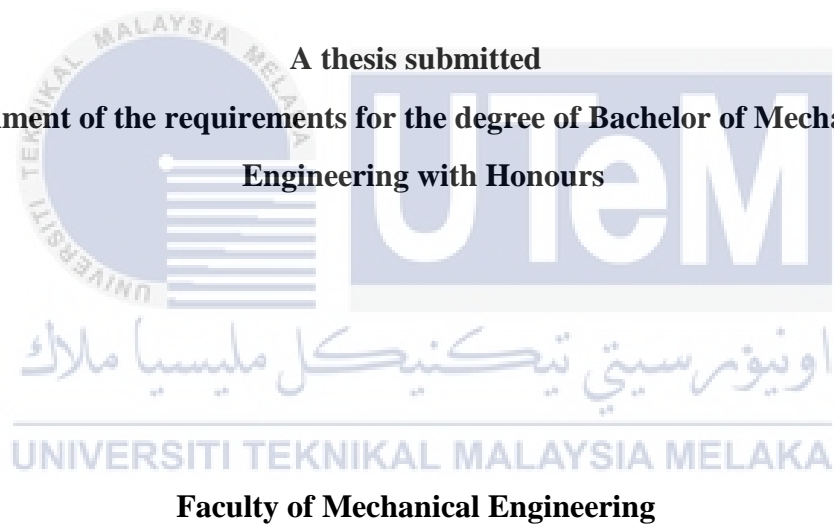


**THE EFFECT OF DIELECTRIC BARRIER DISCHARGE (DBD) PLASMA
ACTUATOR ON THE LEADING EDGE OF AN AIRFOIL**

FAZAL AMSYAR BIN SUZANAN

**A thesis submitted
in fulfillment of the requirements for the degree of Bachelor of Mechanical
Engineering with Honours**



UNIVERSITI TEKNIKAL MALAYSIA MELAKA

2018

DECLARATION

I declare that this project report entitled “Effect of Dielectric Barrier Discharge (DBD) plasma actuator on the leading edge of an airfoil” is the result of my own work except as cited in references.

	Signature	:
	Name	:	..FAZAL AMSYAR BIN SUZANAN..
	Date	:11/5/2018

اونيورسيتي تيكنيكل مليسيا ملاك

UNIVERSITI TEKNIKAL MALAYSIA MELAKA

APPROVAL

I hereby declare that I have read this project report and in my opinion this report is sufficient in terms of scope and quality for the award of the degree of Bachelor of Mechanical Engineering (Hons).



Signature :.....

Name of Supervisor :.....

Date :.....



اونيورسيتي تيكنيكل مليسيا ملاك

UNIVERSITI TEKNIKAL MALAYSIA MELAKA

DEDICATION

To those who have been supporting me throughout my 4 years of study.

Thank you.



ABSTRACT

Dielectric Barrier Discharge (DBD) plasma actuator has been found to be very useful in a wide area of applications. The various types and position of DBD plasma actuator can be applied for specific tasks. For instance, the used of DBD plasma actuator have been implemented on the surface of vehicles such as car and on the wing of aircraft. The DBD plasma actuator used in delay the flow separation occurs toward the surface of vehicles. By applying this method, a higher amount of lift force can be obtained at the critical angle of attack apply towards an airfoil and overcome the increasing drag force. Recently, the aerodynamics performances are frequently being studied for airflow control. The DBD plasma actuator has the ability to control airflow on wing profiles by maintaining the streamline of the boundary layer. This report attempts to define the principle and application of the DBD plasma actuator. DBD plasma actuator is introduced in the beginning a detailed review and designs is presented. Furthermore, for the outstanding findings for this thesis are, actuation case have better aerodynamics performance compared with baseline case and it achieved the functional application of DBD plasma actuator which are used to delay flow separation occurs on the surface of airfoil and prevent stall at higher angle of attack applied. Last but not least this thesis had fulfilled its objectives to investigate the effect of Dielectric Barrier Discharge (DBD) plasma actuator on the leading edge of airfoil and to compare the airfoil aerodynamic performance between base case and actuation case. The angle of attack used in the experiment range from 0° to 24° . The power supply used is 6 KV. The lift coefficient is increase as the angle of attack increases for both cases. The drag coefficient is decreases for actuation case. The experiment is conducted with velocity 15 m/s and 20 m/s. The finding of the study shows that by applying DBD plasma actuator, the value of lift coefficient of an airfoil shows an increment in range of 0.63% to 7.79% with different angle of attack for velocity of 15 m/s. However, the value of drag coefficient of an airfoil shows a declination in range of 3.25% to 100% with different angle of attack for velocity of 15 m/s. For velocity of 20 m/s, the value lift coefficient of an airfoil shows an increment in range of 0.51% to 3.3% and the value of drag coefficient shows a declination in range of 4.9% to 24.4% with different angle of attack. The aerodynamic performance can be improved by applying DBD plasma actuator as the lift coefficient is increase and drag coefficient is decrease based on the result of this study.

ABSTRAK

Penggerak plasma (DBD) amatlah berguna dalam pelbagai aplikasi. Jenis-jenis dan kedudukan penjana vorteks boleh digunakan untuk tugas-tugas tertentu. Antara contoh-contoh penggunaan penggerak plasma DBD adalah diterapkan dipermukaan kenderaan seperti kereta dan di bahagian sayap pesawat. Fungsi penggerak plasma DBD ini adalah untuk melengahkan lagi pembahagian aliran bendalir di permukaan kenderaan. Dengan kaedah ini, daya angkatan dapat di naikkan pada sudut maxima yang ditujukan terhadap aerofoil serta mengatasi daya seretan dihadapi. Sejak kebelakangan ini, prestasi aerodinamik giat dikaji untuk mengawal keberkesanan prestasi aliran udara dan penggerak plasma DBD ini mempunyai kemampuan untuk mengawal aliran udara pada profil sayap dengan kaedah mengekalkan corak aliran bendalir pada lapisan sempadan (Boundary Layer). Laporan ini bertujuan mentakrifkan dasar dan aplikasi penggerak plasma DBD. Bab dimulakan dengan introduksi kepada reka bentuk dan penerangan mendalam mengenai penggerak plasma DBD. Sehubungan dengan itu, penemuan ketara pada tesis ini adalah kes penggerak plasma DBD mempunyai kecekapan aerodinamik yg lebih tinggi berbanding kes yang lain (baseline) dalam kajian ini dan ia mematuhi objektifnya iaitu menyelidik kesan penggerak plasma DBD terhadap permukaan awal di aerofoil dan membezakan prestasi aerodinamik oleh aerofoil antara es baseline ataupun kes actuation. Sudut serangan yang digunakan dalam julat eksperimen dari 0° ke 24° . Bekalan kuasa yang digunakan ialah 6 KV. Koefisien angkat meningkat apabila sudut serangan meningkat untuk kedua-dua kes. Pekali seret adalah berkurangan untuk kes keganasan. Eksperimen dijalankan dengan halaju 15 m / s dan 20 m / s. Dapatan kajian menunjukkan bahawa dengan menggunakan penggerak plasma DBD, nilai pekali angkat an airfoil menunjukkan kenaikan di antara 0.63% hingga 7.79% dengan sudut serangan yang berbeza untuk halaju 15 m / s. Walau bagaimanapun, nilai pekali seretan layang layang menunjukkan penurunan sebanyak 3.25% hingga 100% dengan sudut serangan yang berbeza untuk halaju 15 m / s. Untuk halaju 20 m / s, pekali angkat nilai a airfoil menunjukkan kenaikan dalam kisaran 0.51% hingga 3.3% dan nilai pekali seretan menunjukkan penurunan sebanyak 4.9% kepada 24.4% dengan sudut serangan yang berlainan. Prestasi aerodinamik dapat ditingkatkan dengan menggunakan penggerak plasma DBD kerana koefisien angkat meningkat dan koefisien seretan menurun berdasarkan hasil kajian ini.

ACKNOWLEDGEMENTS

Firstly, Praise to Allah S.W.T for giving me strength and patience for finished this final year project. I would like to express my sincere gratitude to the following person, my project supervisor, Dr. Nazri bin Md Daud for all his assistance, patience, guidance and valuable advice throughout the development of the project. His ideas and wisdom has helped tremendously in constructing the contents of this project. Sincerely a great appreciation indicate to Dr. Md Isa bin Ali and Mr. Faizil bin Wasbari for evaluating my final year project.

I also want to thank to my family especially my mom and dad who always support and give advice to finish my final year project till the end. Then, I would like to thank to my friends who always spend their time with me and also give motivation to me to complete the project from the beginning till the end.

Lastly, thank you to Faculty of Mechanical Engineering as this project really help me to learn a lot about my skills and knowledge that I already earn throughout four years of study in here.

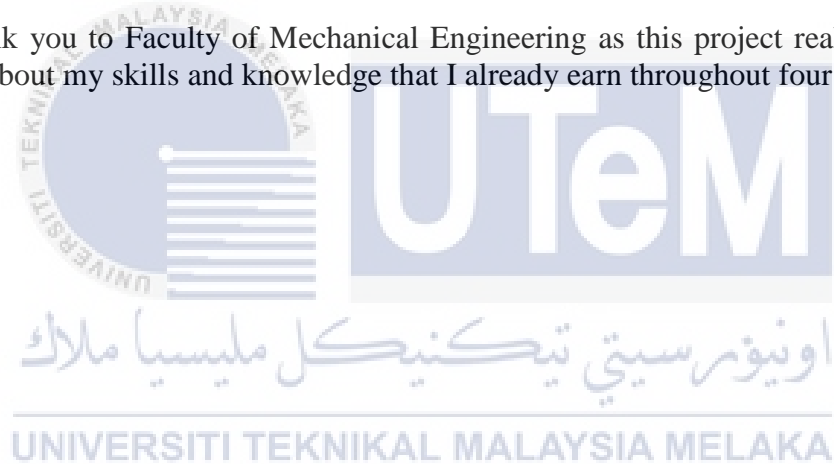


TABLE OF CONTENT

CHAPTER	CONTENT	PAGE
	DECLARATION	
	SUPERVISOR'S DECLARATION	
	DEDICATION	
	ABSTRACT	i
	ACKNOWLEDGEMENTS	iii
	TABLE OF CONTENT	iv
	LIST OF TABLES	vii
	LIST OF FIGURES	viii
	LIST OF ABBREVIATION	xi
	LIST OF SYMBOLS	xii
	LIST OF APPENDICES	xiii
CHAPTER 1	INTRODUCTION	1
	1.1 Background	1
	1.2 Problem Statement	2
	1.3 Objective	4
	1.4 Scope Of Project	4
	1.5 General Methodology	5
CHAPTER 2	LITERATURE REVIEW	7
	2.1 Introduction	7
	2.2 Aerodynamic Application	7
	2.3 Drag force	9

2.4	Lift force	10
2.5	Relation between coefficient of Drag & Lift	10
2.6	Laminar and Turbulent flow	11
2.7	DBD plasma actuator	16
2.8	Experiment on effect of DBD plasma actuator and airfoil performance	24
CHAPTER 3	METHODOLOGY	30
3.1	Introduction	30
3.2	Introduction of DBD plasma actuator	30
3.3	Flowchart	32
3.4	Experimental Equipment	33
3.5	Design drawing	38
3.6	Apparatus setup for Experimental of Wind Tunnel	41
CHAPTER 4	RESULTS ANALYSIS & DISCUSSION	44
4.1	Introduction	44
4.2	Drag Coefficient	44
4.3	Lift Development	45
4.4	Lift Coefficient	48
4.5	Boundary Layer	49
4.6	Experimental of Airfoil (Baseline Case) with speed of 15 m/s sample calculation	51
4.7	Experimental of Airfoil (DBD Plasma) with speed of 15 m/s sample calculation	57
4.8	Experiment of Airfoil (Baseline Case) with speed of 20 m/s sample calculation	62

4.9	Experiment of Airfoil (DBD Plasma) with speed of 20 m/s sample calculation	67
CHAPTER 5	RECOMMENDATION AND CONCLUSION	72
5.1	Recommendation	72
5.2	Conclusion	74
	REFERENCES	76
	APPENDIX A	79



LIST OF TABLES

TABLE	TITLE	PAGE
4.1	Experimental and Calculation Data to Determine C_L and C_D for Baseline Case	54
4.2	Experimental and Calculation Data to Determine C_L and C_D for DBD plasma Case	59
4.3	Experimental and Calculation Data to Determine C_L and C_D for Baseline Case	64
4.4	Experimental and Calculation Data to Determine C_L and C_D for DBD plasma Case	69

LIST OF FIGURES

FIGURE	TITLE	PAGE
1.1	Flowchart for general methodology	6
2.1(a)	Laminar flow consists of isolated layer of air with different Velocities.	12
2.1(b)	Unorganized movements of air molecules of turbulent flow that change the speeds frequently because of the collaborations with one another.	12
2.2	Boundary layer separation over the top surface of a wing.	15
2.3	DBD plasma flow control. Plasma OFF (left), plasma ON (right).	17
2.4	Interest in plasma actuators.	18
2.5	DBD plasma actuator in 1968	19
2.6	Standard SDBD actuator configuration .	21
2.7(a)	Variation of the lift coefficient with the angle of attack when the 1 st ,2 nd , and 3 rd actuators are switched on for Re= 35000.	27
2.7(b)	Variation of the drag coefficient with the angle of attack when the 1 st ,2 nd , and 3 rd actuators are switched on for Re= 35000.	27
2.8(a)	Geometry of NACA 0015.	29
2.8(b)	Geometry NACA 4415.	29

2.9(a)	Mesh generation for NACA 0015.	29
2.9(b)	Mesh generation for NACA 4415.	29
3.1	Flow Chart of the Methodology.	32
3.2	Schematic Drawing of Subsonic Wind Tunnel.	33
3.3	Front view of Subsonic Wind Tunnel.	34
3.4	Side View of Subsonic Wind Tunnel.	34
3.5	Test Section of Wind Tunnel.	35
3.6	NACA 0015 with labels.	36
3.7	Schematic diagram of DBD plasma actuator.	37
3.8	DBD plasma actuator on an airfoil.	37
3.9	A window that appears upon clicking the part design option.	38
3.10(a)	Macros icon in Microsoft Excel.	39
3.10(b)	Run the main file using Macros.	39
3.11(a)	NACA 0015 airfoil model	40
3.11(b)	Views for each sides of Airfoil drawing.	40
3.12	Lift and drag forces measurement against angle of attack at different with velocity.	42
3.13	The test section experiment setup	43
4.1	Drag Coefficient Plotted against Angle of Attack for NACA 23015 Aerofoil	45
4.2	Notation of a Lifting Vane	46
4.3	Two-dimensional Flow around a Lifting Vane	47
4.4	Pressure Distribution for an Airfoil	48

4.5	Lift and Drag Coefficients against Angle of Attack for an Airfoil	49
4.6	Air Velocity at Boundary	51
4.7	Experimental Setup for Baseline Case	55
4.8	Lift and Drag Coefficient Results against Angle of Attack. (Baseline Case)	55
4.9	Lift and Drag Coefficient Ratio against Angle of Attack. (Baseline Case)	56
4.10	Experimental Setup for DBD plasma case	60
4.11	Lift and Drag Coefficient Results against Angle of Attack. (DBD plasma at leading edge) for speed of 15 m/s	60
4.12	Lift and Drag Coefficient Ratio against Angle of Attack. (DBD plasma at leading edge) for speed of 15 m/s	61
4.13	Lift and Drag Coefficient Results against Angle of Attack (Baseline Case) for speed of 20 m/s	65
4.14	Lift and Drag Coefficient Ratio against Angle of Attack. (Baseline Case) for speed of 20 m/s	65
4.15	Lift and Drag Coefficient Results against Angle of Attack. (DBD plasma at leading edge) for speed of 20 m/s	70
4.16	Lift and Drag Coefficient Ratio against Angle of Attack. (DBD plasma at leading edge) for speed of 20 m/s	70

LIST OF ABBEREVATIONS

DBD	Dielectric Barrier Discharge
NACA	National Advisory Committee for Aeronautics
AR	Aspect Ratio
SJA	Synthetic Jet Actuator
STOL	Short Take OFF and Landing
UAV	Unmanned Aerial Vehicles
MAV	Micro Aerial Vehicles
CFD	Computational Fluid Dynamics
3D	Three Dimension

UNIVERSITI TEKNIKAL MALAYSIA MELAKA

LIST OF SYMBOL

α	Angle of attack
C_L	Lift Coefficient
C_D	Drag Coefficient



LIST OF APPENDICES

APPENDIX	TITLE	PAGE
A	Flow Chart	79



CHAPTER 1

INTRODUCTION

1.1 BACKGROUND

Airplanes have made great contribution to the growth of modern society by satisfying many of its needs for mobility in daily life. However, the airplanes should be improved in terms of aerodynamic and any problems that can affect its efficiency can be avoided. One of the alternative ways to improve aerodynamic for an aircraft is by applying the Dielectric Barrier Discharge (DBD) plasma actuator on the airfoil. Plasma actuators are electrical devices that create a divider limited stream without the usage of any moving parts. For aerodynamic applications, the actuators can be utilized as stream control devices to postpone division and enlarge lift on a wing. The standard plasma actuator comprises of a solitary embodied (ground) cathode (Rasool Erfani, Craig Hale & Konstantinos Kontis, 2014).

Previously, the plasma actuators already appeared to be fit for controlling airflow by delivering an electric wind in the limit layer. It used for aerodynamic application for both low and high speeds. Numerous analysts have researched the benefits of this device. As of late, numerous analysts have been learning about flow partition control with unsteady incitation. Be that as it may, the pulse-modulated drive is as yet not obviously depicted when approach is high. Accordingly, an examination on the flow is contemplated when a plasma surface release is driven with pulse modulation both at the slow down control condition and at high angle of incidence condition (Mehul P. Patel, 2008).

The actuator itself is exceptionally basic, comprising of just 2 materials that layered over any surface. As of now, the actuators themselves are lightweight and provided with control from a transformer system that would itself be able to be substantial. As the innovation develops it is normal that the framework weight will diminish, getting to be plainly lighter than that of conventional flow control techniques. The actuator is adaptable and ready to flow the curvature of the surface it is connected to and simple to repair. The actuator can be influenced dynamic or inactive at the flick of a change, to can be actuated at a wide range of balance frequencies and has a high recurrence reaction. The whole framework is all electric and fits in well with the present ethos of airplane makers to deliver every single electric airplane. The current and perhaps the biggest boundary to the usage of this actuators is the impotence to produce momentum that can equal that of ordinary pneumatic systems and be utilized on full scale airplane

1.2 PROBLEM STATEMENT

The airplanes motion is affected by the airfoil's shape. Aerodynamics is associated to airfoil as it is the learning of forces and the subsequent movement of objects through the air. It can affect the efficiency and stability of the airplanes movement. Too many drag forces on the airplanes body could cause high waste in engine energy consumption while too many lift force could cause the airplanes lacks in stability and dangerous. The uses of slat, flap and plasma actuator on an airfoil can improve aerodynamic performance. Slat is a device that install ahead of the wing so air can flow at high angle of attack while flap's location is at the leading edge of airfoil to increase the camber of wing. Vortex generator use to energize the airflow in order to delay the separation of air during high angle of attack.

Besides, the usage of this Dielectric Barrier Discharge (DBD) plasma actuator can contribute in improving performance of aerodynamic. It can be used for many type of vehicles or transportation such as airplanes, car and truck. It usually be applied at the airfoil and blades of airplanes. The working of the actuators relies upon the development of a low-temperature plasma between a couple of unbalanced electrodes by utilization of a high-voltage AC signal over the electrodes. Subsequently, air molecules that surround the electrodes are ionized, and are quickened through the electric field.

This DBD plasma actuator improve aerodynamics as it can increase lift force which enable an airplane to overcome gravity and decreasing the drag force which another aerodynamic force that act as a resistance for an airplane as it moves through air. Lift is a force which opposes the gravity that depends on weight. It produced by dynamic impact of air acting on the wings or airfoil. Lift is affected by the size and airfoil, the angle of attack, and air's density. Lift force produced by a wing is affected by all of them. Force is increase when the air (liquid) moving of the highest part of the wing experiences a hindrance that it must go around and hence its speed increases and its pressure drops. The distinction in pressure between the bottom and upper of the wing brings about more pressure at the bottom, hence pushing the wing upward into the sky.

This actuator is suitable for airfoil in terms of aerodynamic performance. It usually is applied at the leading edge of an airfoil. It can also be used to delay stall which is rapid decreases of lift. When an airfoil exerted air at high angle of attack that exceeds a critical point, a stall is occurred as it is unable to sustain lift. Airflow on the airfoil separates resulting an end of lift. Besides, less number of research on DBD plasma actuator in high angle of

attack have been done. Therefore, this research are implement to investigate the effect of DBD plasma actuator on the leading edge of airfoil and compare the airfoil with plasma actuator and without plasma actuator in terms of aerodynamic performance

1.3 OBJECTIVE

The objectives of this research project are:

1. To investigate the effect of Dielectric Barrier Discharge (DBD) plasma actuator on the leading edge of airfoil.
2. To compare the airfoil aerodynamic performance between base case and actuation case.

1.4 SCOPE

The scopes of this project are:

1. This project focuses on investigation of the effect of applying of Dielectric Barrier Discharge (DBD) plasma actuator by using on the leading edge of airfoil model NACA 0015. This airfoil model NACA 0015 has 6 KV of power and 8 kHz of frequency. This plasma actuator is applied to study the drag force and lift force act on the airfoil. Both forces will influence the performance of aerodynamic for an object.
2. The experimental of wind tunnel with velocity of 15 m/s and 20 m/s on the airfoil. In order to test an aerodynamic for an object, this experiment should be conducted on an

object as it is device for creating a controlled air flow to investigate the movement effects through air and resistance that act on models of aircraft and others object. The object is fabricate in standard design and smaller scale. By conducting this experiment, the result is obtained to know the effectiveness of the object in terms of aerodynamic.

1.5 GENERAL METHODOLOGY

The actions that need to be conducted to achieve the aims in the research are listed below:

1. Suitable Objective, Scope and Problem Statement

Study the objective, scope and problem statement of the project.

2. Literature review

Journals, articles or any sources regarding the research will be reviewed.

3. Study the DBD plasma actuator application on airfoil and basic principle DBD.

The theory regarding of DBD plasma actuator application on airfoil and basic principle DBD is learned and well understood.

4. Experiment of Wind Tunnel

The wind tunnel test will be conducted on fabricated airfoil to study the effect of DBD plasma actuator in terms of aerodynamic performance

5. Analysis and proposed solution

Analysis will be done to know the efficiency of the DBD plasma actuator applied on the leading edge of airfoil.

6. Report writing

This research will be written in a report at the end of this study.

The methodology of this study is summarized in the flow chart as shown in Figure 1.1.

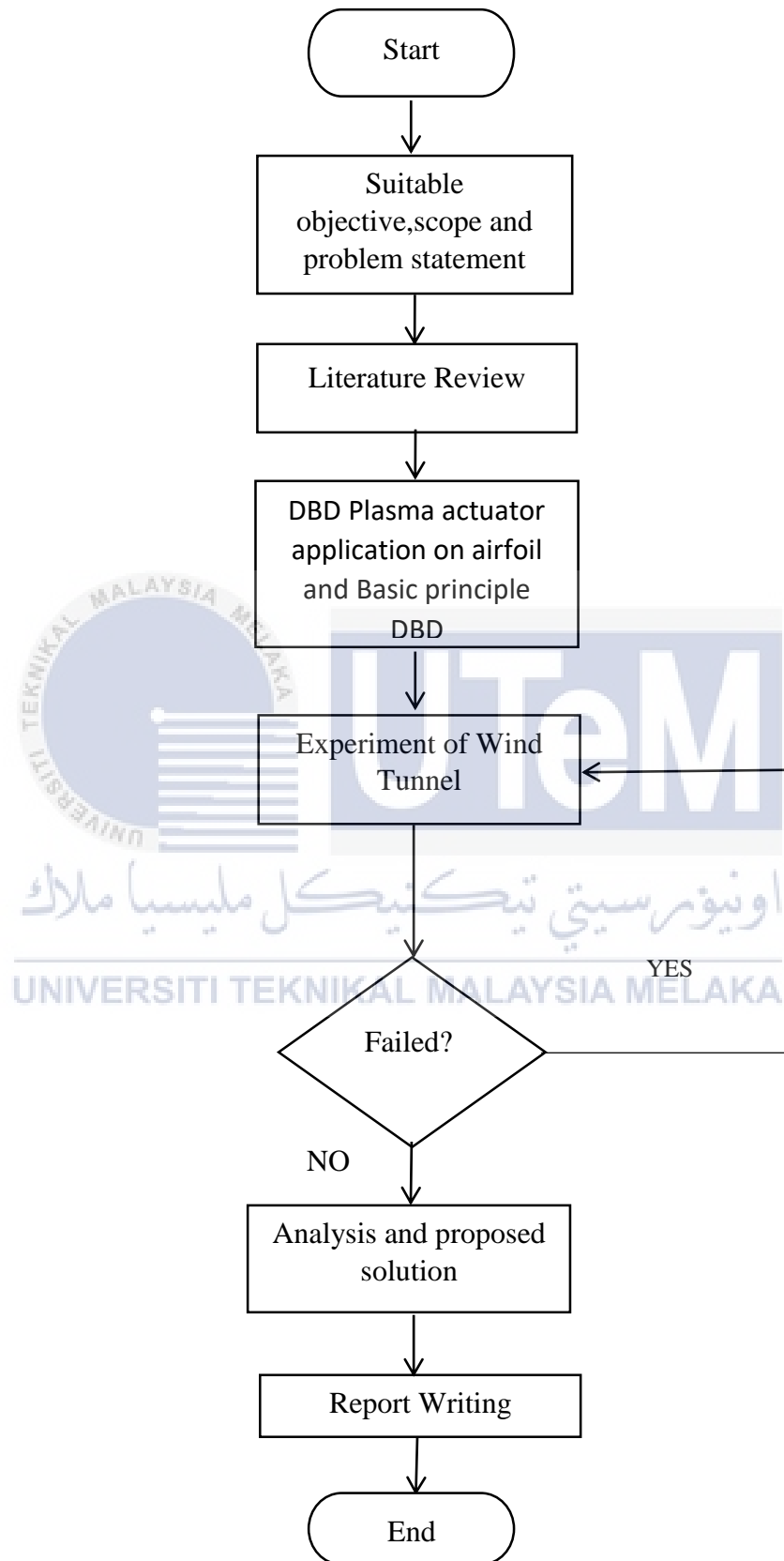


Figure 1.1: Flowchart for general methodology

CHAPTER 2

LITERATURE REVIEW

2.1 INTRODUCTION

For the literature review, the structuring of the chapter includes the Dielectric Barrier Discharge(DBD) plasma actuator which cover the literature regarding aerodynamic application and how it works in aircraft. The drag and lift forces concepts are also included in this chapter. Other than that, this chapter also includes DBD plasma actuator background which describes about the history of this plasma actuator. Next, it also includes effect of DBD plasma actuator for vehicle which describe the usage of DBD plasma actuator for vehicle. Besides, efficiency of DBD plasma actuator, component and how it works also will be included in this chapter.

2.2 AERODYNAMIC APPLICATION

The research regarding the interaction of gases among moving bodies is known as aerodynamics. Since the gas that we experience most is air, aerodynamics is essentially concerned about lift and drag forces. The airflow will pass over and around solid bodies. The principles of aerodynamics is applied by engineers to design of a wide range of things, including structures and bridge but mainly used for vehicles such as aircraft and automobiles. The design of vehicles is very prominent as it can affect the aerodynamics because it associated to the forces (lift and drag)..

2.2.1 DRAG CONCEPT

Drag in general physics is referred or defined as the resistive force that experienced by an object/ body when it is in motion with respect to the fluid surrounding it. Drag forces are rely upon the velocity of the object and is shown by a formula defined as:

$$F_D = \frac{1}{2}\rho v^2 C_D A \quad (2.1)$$

Where F_D is the drag force

ρ is the fluid density

v is the velocity of the object in the fluid

C_D is the drag Coefficient

A is the cross sectional area

Drag force is highly rely upon the density of the fluid, velocity of the object and cross sectional area of the body acting with the fluid. The sleeker the body will produce lower value of drag coefficient (which is a dimensionless value) and less is the drag force is. Despite that, the drag force is proportional towards the density and velocity. It is useful as the net force exerted on the horizontal direction on the aircraft can be calculated as well as viscous forces.

2.3 DRAG FORCE

The drag force is against the travelling car's motion which already explained in 2.2.2. This ultimately affects performance of the car, economy of fuel as well as greater power is required to overcome the force. As usually given by the expression in which is

$$F_D = \frac{1}{2}\rho v^2 C_D A$$

A: "A" is the frontal area in square of meter (m²). The vehicle's size is identified directly with the properties of drag and is described by the value of **C_DA**. However the frontal area is slightly less than the total width & length of the car measured in (m²)

C_D: Coefficient of Drag is a function of Shape, Reynold number (Re), Mach number (Ma), Froude number (Fr) and relative roughness ϵ/l and is given mathematically by:

$$C_D = \phi(\text{Re, Ma, Fr, } \epsilon/l) \text{ (Munson, 2006)}$$

The density of the air ρ is dependent on the temperature, humidity, altitude and pressure. On in any standard condition the density of the air is 1.23 kg/m³.

The term $\frac{1}{2}\rho v^2$ is the dynamic pressure of the air and v is the final velocity of the vehicle.

2.4 LIFT FORCE

Other than the Drag force, there is one more component of the force called the Lift force which tends lift the aircraft and reduces the friction between the air and body of aircraft.. This means the force acts as the stability of the aircraft and handling too. Given by the eqn 1, $F_L = \frac{1}{2}\rho v^2 C_L A$, lift force plays a significant role in the aerodynamic optimization of the car. The lift force is a relies upon the shape of the aircraft. In the present modern day passenger aircraft, the coefficient of lift ranges from 0.3 – 0.5 for any wind angle at 0° (Hucu, 1998). For opposite air direction, the lift coefficient C_L can vary from 1 and increases on.

2.5 RELATION BETWEEN COEFFICIENTS OF DRAG & LIFT

Before we study and the application of the coefficient, from an experimental study of a generic aircraft, it was concluded that the lift and drag coefficient for the flow around the body of the aircraft is predominantly relies on the slant angle. It was observed with the generic model from 0° to 29° the development of the lift is straight and definitely changes to negative as the angle comes to 30°. The drag coefficient is least at 15° angle which implies the lift coefficient is near zero and ends up 50% greater when the inclination angle achieves 29°.

However past the inclination point of 30° the lift and drag turns out to be about steady. (Ivan Dobrev, Fawaz Massouh, 2014).

2.6 LAMINAR AND TURBULENT FLOW

Laminar Flow is the smooth, continuous stream of air over the form of the wings as shown in figure 2.1(a), fuselage, or different parts of an air ship in flight. Laminar flow is frequently found at the front of streamlined body and is an essential factor in flight. If the laminar air flow over a wing area is interrupted, turbulence is produced which brings about lost lift and a high level of drag. An airfoil intended for least drag and continuous stream of the limit layer is known as laminar airfoil.

The theory of laminar flow managed the advancement of a symmetrical airfoil area which had a similar curvature and flow on both the bottom and top surface. The design was generally thin at the leading edge and logically enlarged to a state of most greatest thickness as far as possible. The theory in utilizing an airfoil of this design was to keep up the bond of the limit layers of airflow which are available in flight as far towards the leading edge if possible. The boundary layer would be hindered at high speeds and the resultant break that would produce a turbulent flow will flow through the airfoil . This turbulence would be acknowledged as drag up the point of most extreme speed, at which time the aircraft flying attributes and control surfaces would be influenced. The development of the limit layer is a procedure of layers of air formed one by the other. The term of laminar is gotten from the derivation of laminar principle included.

The flow lines are not organized is called turbulent flow as shown in figure 2.1(b). Airfoil travelling through a fluid can cause the flow separation. For this situation, the turbulence that is produced behind the airfoil is known as a wake. Extremely turbulent wakes happen behind moving airfoil in air. The impact of the turbulent wake is bring down the

settling speed of the the particles due to one part of the fluid movement from the eddy is oppose the particles movement in direction, and also drag force is on the particles is exerted (Imad Shukry Ali & Sahab Shehab Ahmed, 2011). Besides, the turbulent flow will cause the different in momentum. This is due to the transition of higher energy particles give it momentum to the lower energy particles.

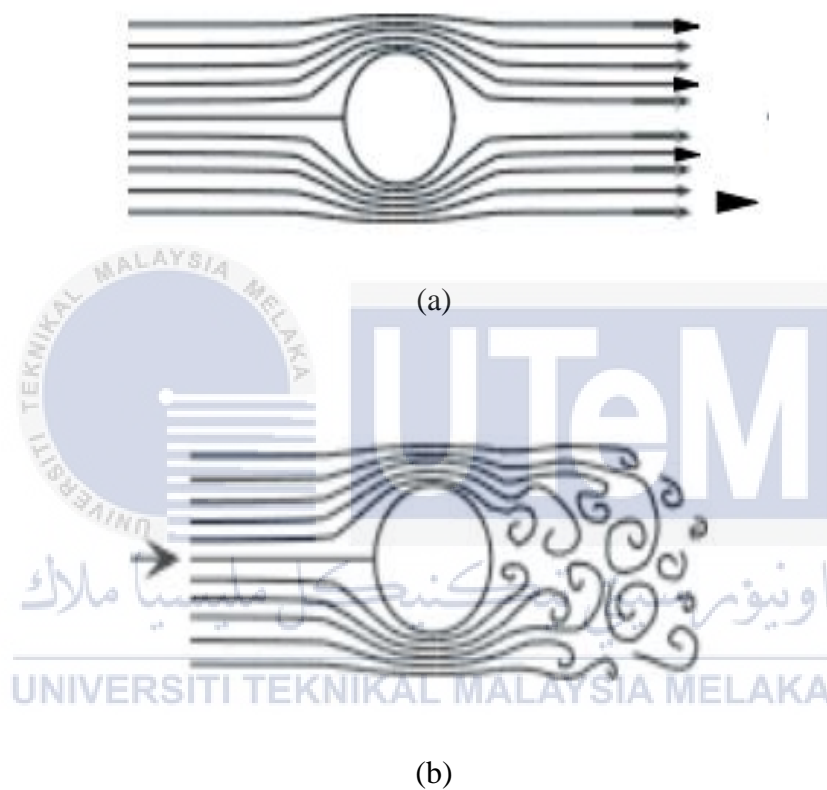


Figure 2.1: (a) Laminar flow comprises of isolated layer of air with various velocities; (b) Unorganized movements of air molecules of turbulent flow that change the speeds frequently because of the collaborations with one another..

(http://nautilus.fis.uc.pt/personal/pvalberto/aulas/cef_mestrado/Air.Resistance.pdf)

On the other hand, one of the prominent parameter of this airfoil experiment is Reynolds number. Boundary layers might be either turbulent or laminar contingent upon the estimation of the Reynolds number. The boundary layer is laminar and the streamwise speed changes consistently as one moves far from the wall for the lower Reynolds numbers. The boundary layer is turbulent for the higher Reynolds numbers and the streamwise speed is portrayed by unsteady whirling streams inside the boundary layer. The outside stream responds to boundary layer edge similarly as it would to the physical surface for an object. So the boundary layer gives any object a “powerful” shape which is not same as the physical shape.

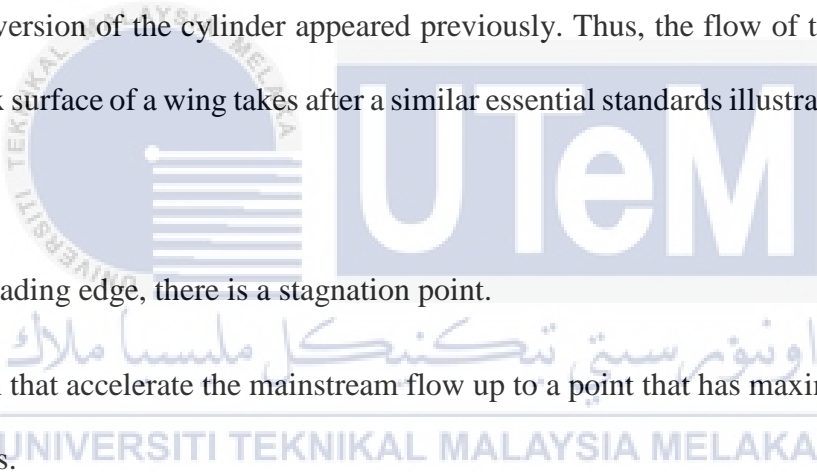
2.6.1 DELAY IN FLOW SEPARATION

The flow separation happens on the wing of aircraft as the boundary layer goes sufficiently far against an adverse pressure gradient. The particles's speed that clearly closest to the surface falls about to zero. The boundary layer flow ends up noticeably isolates from the surface and rather takes the types of swirls and vortices and results in enlarged drag, especially pressure drag. This paper clarifies the curiosity of the synthetic jet actuator (SJA) towards accomplishing the reattachment of boundary layer partition and, consequently, the wing of an aircraft is controlled by the flow separation.

By utilizing the SJA, the jet is blended from the surrounding fluid using forced periodic excitation of the diaphragm to deliver a train of consecutive streamwise vortices that cooperate with the boundary layer and also change the momentum with the less energetic close fluid wall. The vortical structures are created over a more extensive scope of length and timescale, and their restrictive qualities make them alluring fluidic actuators for various

flow control applications (Smith et al, 1999) and (Mallinson et al, 1999) utilized piezoelectric diaphragm actuators, since they are easy to construct and could be worked over a more extensive scope of recurrence. In this work, the piston type actuator is utilized, as the primary concentrate is on the development of the vortical structures and thier ensuing collaboration with the boundary layer.

For the wings of aircraft, boundary layer separation can prompt exceptionally huge outcomes going from an expansion in pressure drag to a dramatic loss of lift, known as stall of aerodynamic. The state of an aircraft wing is basically a prolonged and maybe deviated asymmetric version of the cylinder appeared previously. Thus, the flow of the air over the upper convex surface of a wing takes after a similar essential standards illustrated previously.

- 
- At the leading edge, there is a stagnation point.
 - A region that accelerate the mainstream flow up to a point that has maximum thickness.
 - A region that decelerate the mainstream flow above the point of maximum thickness.

The summarization of these three points are shown in the schematic diagram below.

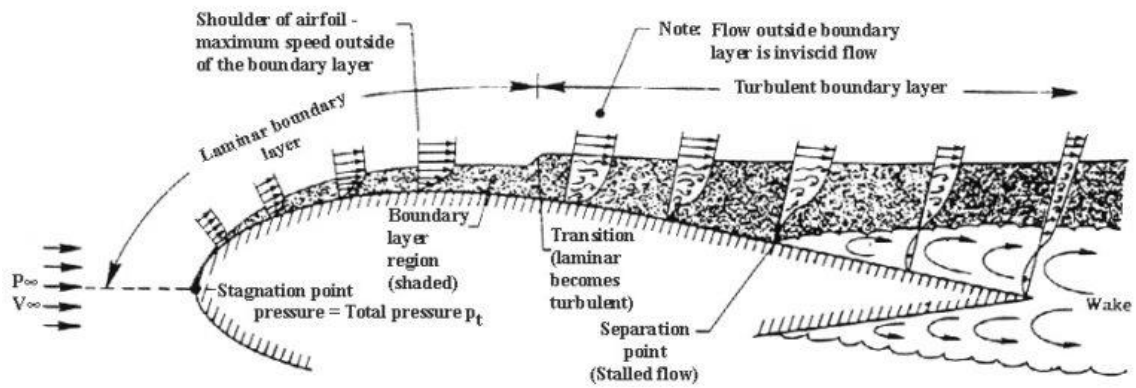


Figure 2.2: Separation of boundary layer over the top surface of a wing.

(<http://aerospaceengineeringblog.com/boundary-layer-separation-and-pressure-drag/>)

Boundary layer separation is very prominent issue for the wing of aircraft as it actuates a huge wake that totally changes the flow downstream of the separation point. Skin-friction drag arises because of the inherent fluid viscosity. The fluid adheres to the wing's surface and the related frictional shear stress that exerts a drag force. At the point when a boundary layer isolates, a drag force is instigated because of contrasts in pressure upstream and downstream of the wing. The general measurements of the wake, and subsequently the extend of pressure drag, relies upon the separation point along the wing. The velocity profiles for both boundary layers (see picture above) demonstrate that the speed of the fluid become much slower as it far from the wall for the laminar boundary layer. This will result in reverse direction of the flow for laminar boundary layer substantially prior within the sight of an adverse pressure gradient compared to the flow in a turbulent boundary layer.

2.7 DBD PLASMA ACTUATOR

Dielectric Barrier Discharge(DBD) plasma actuator acts as a flow control that including in manipulating a flow to get a required change. It means that this actuator able to modifying the flow from laminar to turbulent transition in particular boundary layer and can prevent flow separation. By applying this plasma actuator, lift force can be increased and the drag of an airfoil can be reduced, improving in mixing or reducing acoustic noise. It is of best useful significance for aerospace industry, business and military flight, vitality frameworks, vehicle industry, and wherever where outer and inner wind currents happen. There are a few systems through which the flow can be controlled. Control over laminar-to-turbulent progress can be exceptionally valuable. For instance, in certain cases the turbulent limit layer can have a request of greatness higher skin friction drag than the laminar one. For aircraft and autos concealment of change implies better fuel proficiency, longer ranges, and higher velocities.

The scope of operational conditions for a wind turbine, take-off and landing velocities of aircraft, mobility of a fighter jet are exceedingly influenced by greatest lift and stall attributes of the airfoil. The created lift relies upon the capacity of the flow to take after the curve and increments with the angle of attack and camber of the wing. Sooner or later however the stream neglects to take after the bend and isolates. In this way concealment of limit layer partition is one of the principle open doors for stream control. Another imperative issue is the acoustic noise produced by turboprops, helicopters, autos, wind turbines (infra solid), and so on. It is related with nature of turbulent of many flow and is a region where flow control can have a remarkable effect. In a few conditions turbulence is wanted since it upgrades mixing and here once more, the flow control can assume a vital part.

There are also some parts which are not mentioned in detail but are inferred such as optical diagnostics, electrodynamics and also high voltage electronics. To prevent from spreading out our endeavors to these parts of engineering and science, we focused for the most part on the DBD plasma part, remembering that its application would be for flow control.

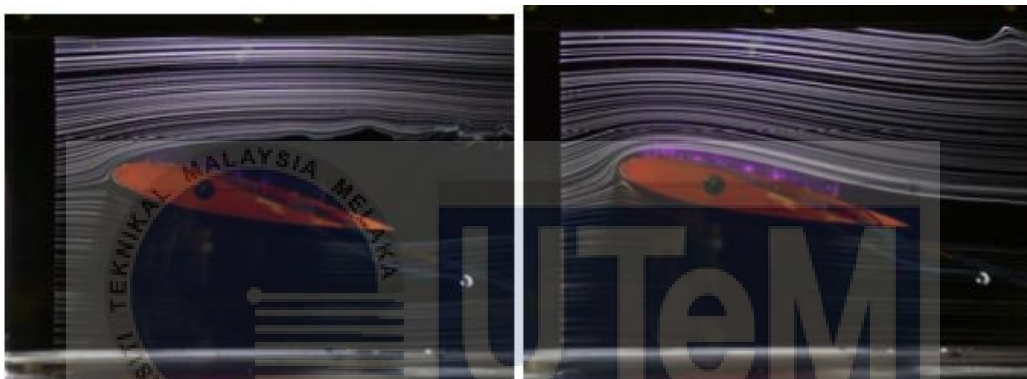


Figure 2.3: DBD plasma flow control. Plasma OFF (left), plasma ON (right).

(<https://ntrs.nasa.gov/archive/nasa/casi.ntrs.nasa.gov/20120015252.pdf>)

UNIVERSITI TEKNIKAL MALAYSIA MELAKA

2.7.1 BACKGROUND

The tale of DBD plasma actuators for flow control started in 1998 when Reece Roth from Tennessee University introduced his initially paper on DBD flow control (J. Reece Roth, Daniel M. Sherman, 1998). His exhibit of DBD flow control capacities is appeared at Figure 2.3, where he exhibited that partition at high angle of attack can be stifled. The benefit of plasma actuators are their power, simplicity, light weight, low control utilization, and sufficiently quick reaction time to make them equipped for real time flow control.

Since 1998, enthusiasm for DBD plasma actuators has been developing exponentially as is represented by number of Google hits on "plasma actuator" at Figure 2.4. In any case, understanding of the fundamental material science is inadequate, and, albeit a few methodologies have been appeared to enhance the performance of plasma actuators, just a total comprehension of both plasma forms and their collaboration with the flow will permit improvement of the performance. It is the aim of this paper to research components of DBD plasma actuator flow control and propose advance changes to it.

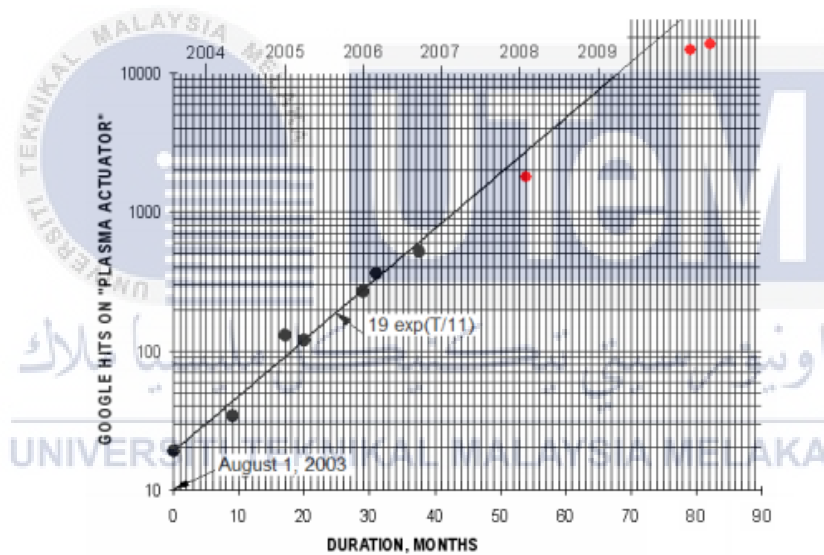


Figure 2.4: Interest in plasma actuators.

(<https://ntrs.nasa.gov/archive/nasa/casi.ntrs.nasa.gov/20120015252.pdf>)

The introduction would not be finished without specifying that, despite the fact that DBD plasma actuators were acquainted with current open by R. Roth, they were known back in the sixties in Soviet Ukraine (J.Reece Roth, 1998). Figure 2.5 demonstrates a schematic of one of those tests. The setup is marginally not the same as the one proposed by Roth. The

electrode is flush mounted on the airfoil and the divided base terminal comprises of a few wires installed into the fold. Notwithstanding this distinction, the result of separation control and plasma induced flow velocities were same to those obtained nowadays. The reason the innovation has been overlooked was most likely in light of the fact that at those circumstances most endeavors were spent on super-and hyper-sonic flights, and the plasma induced flow of the requests of 10 m/s did not look that amazing all things considered

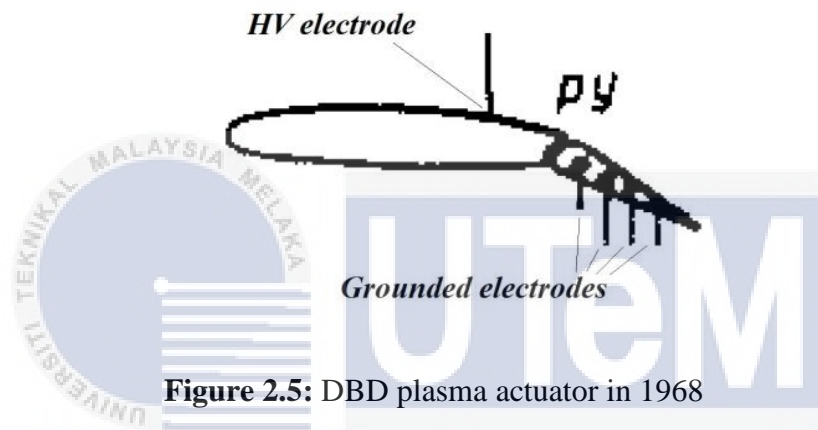


Figure 2.5: DBD plasma actuator in 1968

(<https://ntrs.nasa.gov/archive/nasa/casi.ntrs.nasa.gov/20120015252.pdf>)

UNIVERSITI TEKNIKAL MALAYSIA MELAKA

2.7.2 DEVELOPMENT OF DBD PLASMA ACTUATOR

The control of the flow over aircraft has been the subject of serious research as the suitable arrangement can yield an awesome number of advantages. Such systems concentrate on the control of the limit layer, a thin layer found near the wall of an object going through a liquid. Increase in lift performance and drag reduction can be occurred as this region is successful controlled. These thus take into account bring down take-off and landing speeds, shorter runways, expanded continuance, enhanced mobility and also bring down fuel utilization. The expenses is not the benefits of flow control but its proficient to contend

directly with the tough and altogether innovation of the traditional aircraft flow control that already proved such as flaps and slats.

Lately, the investigation regarding a new technique for flow control has been done that may has the potential in aircraft technologies. It is known as the single dielectric barrier discharge (SDBD) plasma actuator (T.C Corke, C.L Enloe, & S.P Wilkinson, 2010). It consists of two electrodes offset in the clockwise direction and divided by a dielectric layer. One of the electrodes is connected to the earth and the other one that which is exposed electrode is attached to a high voltage supply. As it is activated, the plasma that glow in purple color is visible, originating at the exposed electrode and disperse out across the surface of dielectric that is placed on top of the encapsulated electrode as shown in Fig. 2.6. The air is ionised by the plasma consists of electrons and ions with the bulk plasma reveal electrical neutrality.

The best part of this arrangement is it can deliver jet that flow away from the exposed electrode over the encapsulated in a short period of time, without the requirement for any moving parts. This actuator is light weight, simple to repair, adaptable and capable to follow the surface of curvature it is connected to. It can be turned on or off or inactive at the flick of a switch, can be initiated at an extensive variety of tweak frequencies and has a high frequency response. The whole framework is all-electric and fits in well with the present ethos of aircraft manufacturer to create every single electric aircraft.

Several studies have been done in order to optimize the DBD plasma actuator on its effect in improving aerodynamic performance. There are several variables that affect the intensity and plasma distribution such as frequency, electrode configuration, voltage waveform, dielectric material and thickness. In present, this actuator lacks in the induced momentum as directly compared with pneumatic systems. Further study of the plasma actuator mechanism for production of jet or techniques to improve the momentum addition are significant to establish the plasma actuator as a rightful technique for flow control. The plasma actuator has to be optimized and maximum induced velocity needs to be increased (Erfani, Zare-Behtash, Hale, & Kontis, 2015).

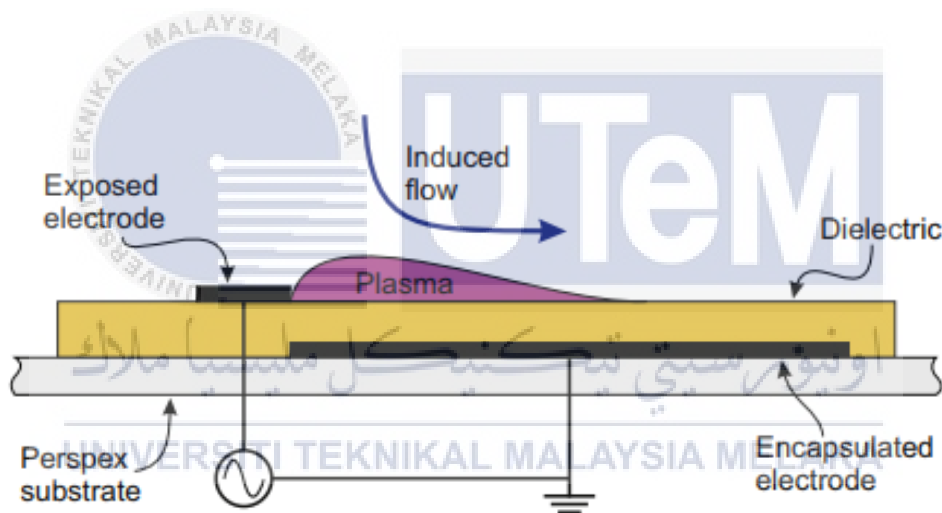


Figure 2.6: Configuration for the Standard SDBD actuator.

(Erfani, Zare-Behtash, Hale, & Kontis, 2015)

Boundary layer of flow control can be defined as “It can include any mechanism or process through at which the layer of the boundary of a fluid flow is caused to react differently from its normal which the flow naturally flows along a straight surface. The first one to be aware regarding the importance of the boundary layer for entire flow in 1904 is Ludwig

Prandtl. He was also delaying separation of the cylinder surface by using boundary layer suction. The common boundary layer control methods are shown below:

1. **Boundary layer bleed.** Start with boundary layer suction which is a first method that has been used by Prandtl in his original experiment. The flow separation can be occurred due to presence of adverse pressure gradients. It flow direction through the surface can be reversed when boundary layer loses its momentum because of the viscous effects. The part of boundary layer that has low in momentum can be withdrawn from the flow using discrete suction slots and porous surface which can caused the profile fuller. This technique has been proven that can suit for both low and high speeds which all the remaining problems are maintained and reliable of the suction surfaces.
2. **Boundary layer blowing.** This method is quite same with the previous one. The boundary layer is controlled using discrete slots on the wall. The velocity profile that made fuller by direct tangential air injection at high velocity along the surface. This control method also has been applied in military sector and STOL transports. Even though the it is less efficient compared to suction, this blowing needs less interior ducting.
3. **Passive vortex generators.** It is small in aspect ratio airfoils mounted directly to the surface of a wing. This vortex generator create stream wise vortices that can circulate the retarded near wall flow that free in stream flow resulting the velocity of near wall flow increase. This control technique is passive as it does not need any power source to make it function and is always ON. Besides, it leaves many opportunities for improvise or optimization as the position of this generator on wing of airplane or turbine blade can

be chose freely. This vortex generator are widely used in almost every modern commercial airplanes.

4. **Acoustic excitations and periodic forcing.** It is a control technique for the active boundary layer. This technique depends on triggering laminar to turbulent transition, but it is differs from other which can be applied any time needed. The sound of a certain frequency and intensity can give effect to the boundary layer. The acoustic waves can be found either be internal which is mounted on the surface or external which is outside of the boundary layer. The periodic forcing method is also effective as it achieved the best control at certain frequencies that are usually found to happen at a Strouhal number, $St = f c / U_{\infty}$ (f is a frequency, c is the length of chord, U_{∞} in the free flow velocity), near unity.

5. **Boundary layer turbulizer.** It is a technique to trip boundary layer by using rough or groves surfaces. It is also can also trigger the transition from laminar to turbulent. A laminar boundary layer is less resistant to separation compared to the turbulent one. For a turbulent boundary layer, the momentum transfer in the layer is strongly enhance because of the presence of eddies in the flow. The separation will be delayed and also result in the velocity profile fuller.

2.8 EXPERIMENT ON EFFECT OF DBD PLASMA ACTUATOR AND AIRFOIL PERFORMANCE

Based on previous research, the aim for developing this Dielectric Barrier Discharge (DBD) plasma actuator is to study the effect of this plasma actuator in airfoil performance. The effect of this actuator in terms of lift and drag at different locations is studied. This research also shows the present information concerning on the electric wind induced by DBD plasma actuator in inactive air at atmospheric pressure. For high lift airfoil, the control of separation of flow is researched utilizing single DBD plasma actuator. (Little, Nishihara, Adamovich, & Samimy, 2010). The experiment has been conducted by using NACA 4415 airfoil model. The plasma actuator is applied at the leading edge of the airfoil, at 30% and 60% of the length of chord. This model is manufactured using Plexiglas material with a span b of 158 mm and a chord c of 100 mm. Three DBD plasma actuators are used for this experiment that mounted on a NACA 4415 airfoil model. The actuator has thickness of 0.066 mm and made using copper material. The exposed electrode placed at the leading edge is known as baseline electrode while the two placed downstream. The dielectric within the buried electrode and the exposed electrode are made of PCB that supported by 1mm thickness and two layers of Kapton sheet of 76.2 μm and 125 μm . The experiment is to study the relation between the the position of the actuators and the the lift generated as it is turned on.

The experiments are conducted at a velocity of 5 kHz and at $Re=35000$. The angle of attack α is varies from -6° to 16° . The streamwise are aligned with two axes and vertical direction of the wind tunnel in order to measure the lift and drag forces generated by the model. The recording sequence are divided into two which are with actuation and no actuation. The first 2 seconds is for no actuation to define the baseline flow and then followed

by 4 with presence of actuation on the model. The sampling frequency is about 1 kHz and the signal is low pass filtered which is at 10 kHz. It is set at the frequency as to remove vibrations effects that induced by the flow.

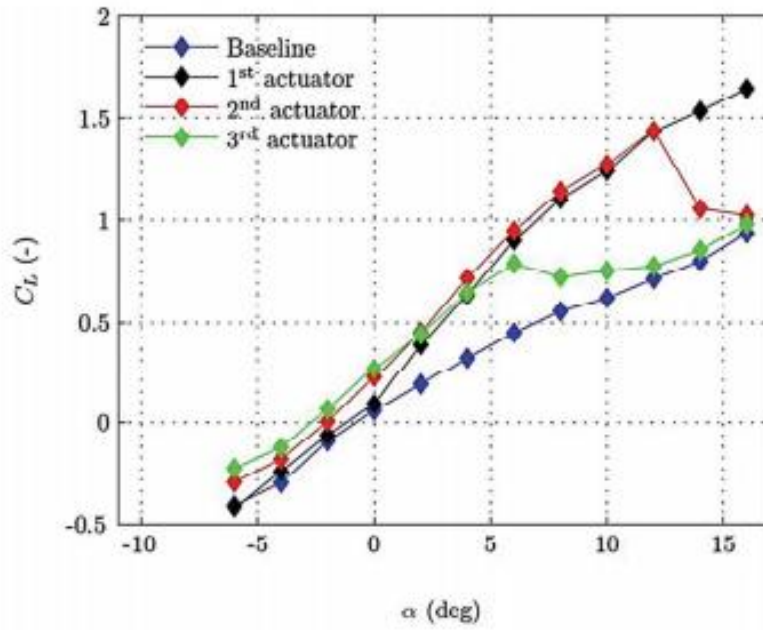
2.8.1 RESULTS AND DISCUSSIONS

In this section, the result of the experiment is obtained. This experiment also is conducted to characterize the drag and lift coefficients as the actuators that located on the airfoil are activated one by one. the force measurement are used. The purpose of this experiment is to determine which DBD plasma actuator will produces the best drag and lift coefficient for a given angle of attack. Besides, the experiment also been done to determine the correlation between the location of the plasma actuators and the angle of attack. Based on the figure 2.7 (a)-(b) , it shows that the variations of the lift coefficient C_L and the drag coefficient C_D with α as the actuators are activated for $Re= 35000$. The first actuator is located at leading edge (black line) while the second actuator (red line) and the third actuator (green line) are placed at 30% and 60% of the length of chord. Based on figure 2.7 (a)-(b), the blue lines indicate the baseline conditions when no actuator are activated. The α range from -6° to 16° for different actuators are globally increase the value of C_L of the airfoil model especially a maximum improvement by the third actuators with almost 4 times the baseline value $C_L=0.0570$ that obtained at $\alpha= 0^\circ$.

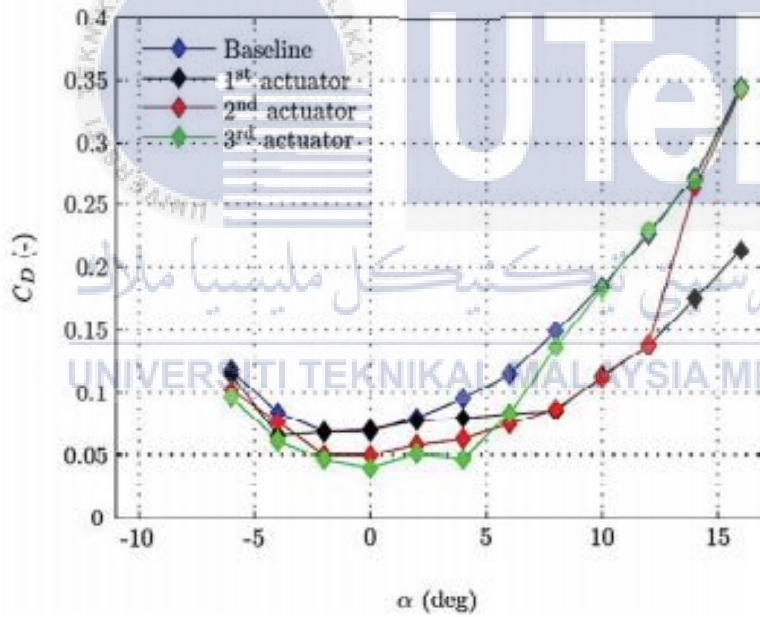
For the angle up to 0° , the third actuator produces a higher lift coefficient that other actuators while for the angle between the 2° and 10° , the second actuator (red line) generates the highest value of C_L . The first actuator (black line) generates the highest lift coefficient at the high angles of attack that range from 12° to 16° . At the angle of -6° , the largest lift

coefficient has been produced by the third actuator with a value that slightly more than 44% the value of the baseline while at angle of 16° , the best lift coefficient has been produced by the first actuator with an improvement of 75.7% of the baseline value. Thus, the location of the actuators are associated with the best C_L that near to the leading edge with increase in value of angle of attack (α).

The plasma that is generated by the third actuator produces the lowest drag up to 4° compared to other actuator as shown in figure 2.7 (b). As the plasma from the second or first actuator is turned on, the airfoil has almost equal value of drag coefficient which is $C_D=0.138$ and 0.139 at angle of attack up to 12° for both actuators. As the first actuator is switch on, the value of drag is lower at above 12° . Based on the experiment, the trend of the drag and lift produced by the three actuators are quite same with about the same actuators producing the best drag and lift coefficient within the equal range of angles of attack even for certain angles, the actuator generating the lowest drag will not certainly will generate the best lift. From figure 2.7 (a)-(b), it can be seen that the best drag and lift coefficient are obtained from actuators that located nearer to the leading edge as the angle of attack increases (Bouremel, Li, Zhao, & Debiasi, 2013)



(a)



(b)

Figure 2.7: Variation of the lift coefficient and the drag coefficient with the angle of attack when the 1st, 2nd, and 3rd actuators are switched on for $Re = 35000$:

(a): C_L ; (b): C_D . (Bouremel, Li, Zhao, & Debiassi, 2013)

2.8.2 NACA 0015 & NACA 4415 AIRFOIL

NACA 0015 is a type of airfoil model. This airfoil is symmetrical and have no chamber. The digit 15 indicates the thickness of the airfoil is about fifteen percent to chord length proportion. The NACA 4415 airfoil model has a camber of four percent which located forty percent from the main edge with fifteen percent of maximum thickness. Both airfoil model is tested to include drag, lift, velocity contour, pressure and also the transient progression for flow separation. The tests and experiment for airfoil has been done by many scientists. Lately, examination enthusiasm for the airfoil execution has resuscitated by Unmanned Aerial Vehicles (UAVs) and also Micro Aerial Vehicles (MAVs) (Katam, 2005). The degree for the wing airfoil bended is same for both the top and base side. Based on the focal point of the main edge to the trailing edge one, a line is drawn make the both upper and lower part of the airfoil symmetrical. The NACA 0015 profile is suitable for baseline airfoil (Wen-Chao, 2012).

Symmetrical NACA 0015 airfoil model utilized by wind turbine cutting edge (Ragni & Ferreira, 2014). NACA 4415 airfoil model has a impact which can decrease the level of degree of flow separation that is shown by Jamey and David whom working the oscillation for the top surface of an airfoil. The shape of the airfoil should be considered as the lift and drag of the airfoil is affected by surface finish condition (Abbott, 1945). The integration of pressure distribution around the airfoil can determine the drag and lift coefficient thus friction effect is underestimated and can lead to error (Zhang & Igarashi, 2011). For simulation of the airfoil, the CFD simulation is used. The coordinates for both airfoils is imported and the geometry is created to be used for the simulation as shown in Figure 2.8(a) and 2.8(b). The flow domains are divided into smaller subdomains to analyze the flow of the

fluid (Diniesh K.G & Vignesh, 2013). Subdomains of the flow that made up of geometric primitives such as hexahedra and tetrahedral in 3D while quadrilaterals and triangles in 2D (Cousin, H.S & Torres, 2015). Besides, mesh analysis is conducted and the relevance center is assume as fine and in C-mesh domain smoothing is high as shown in Figure 2.8(c) and 2.8(d) (Rubel, Uddin, Islam, & Rokunuzzaman, 2016)).

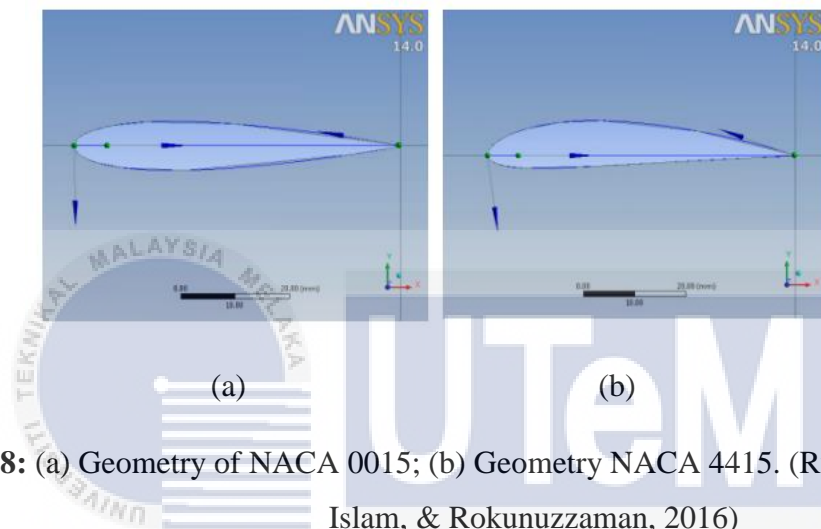


Figure 2.8: (a) Geometry of NACA 0015; (b) Geometry NACA 4415. (Rubel, Uddin, Islam, & Rokunuzzaman, 2016)

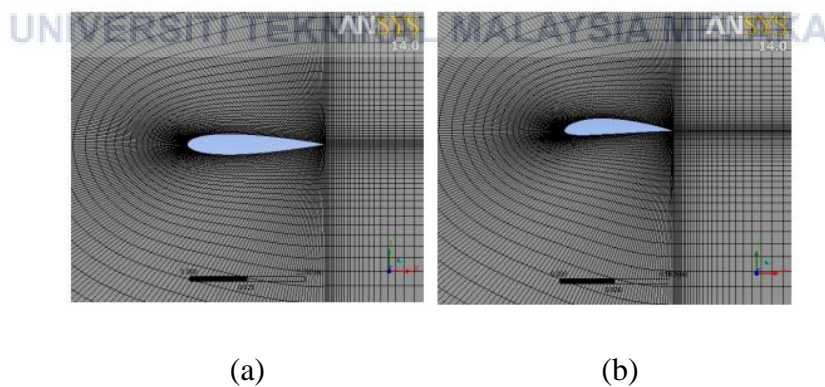


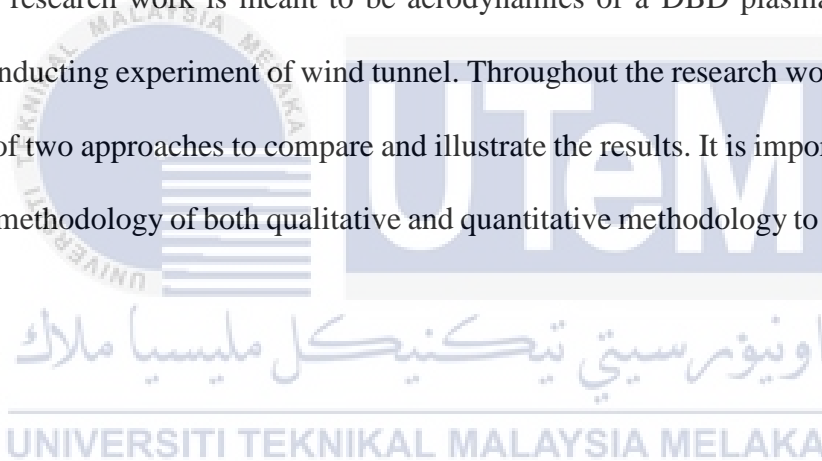
Figure 2.9: (a) Mesh generation for NACA 0015; (b) Mesh generation for NACA 4415.(Rubel, Uddin, Islam, & Rokunuzzaman, 2016)

CHAPTER 3

METHODOLOGY

3.1 INTRODUCTION

The research focuses on the application of the DBD plasma actuator on the airfoil. Hence it was important to discuss the vital aspects of the aerodynamics involved in the airfoil and the effect of the DBD plasma actuator on the aerodynamics of the aircraft in the literature review. The research work is meant to be aerodynamics of a DBD plasma actuator on a airfoil by conducting experiment of wind tunnel. Throughout the research work there will be application of two approaches to compare and illustrate the results. It is important to have an appropriate methodology of both qualitative and quantitative methodology to obtain the final result.



3.2 INTRODUCTION OF DBD PLASMA ACTUATOR

DBD plasma actuator are varies in design and geometries. The main purpose of this research is to investigate the effect of Dielectric Barrier Discharge (DBD) plasma actuator on the leading edge of airfoil. Comparison between the airfoil with plasma actuator and without plasma actuator in terms of aerodynamic performance. This methodology applied in this study is based on experimental study on the effect of DBD plasma actuator at the leading edge of airfoil. The NACA 0015 model airfoil is used in for this experiment. The air velocity is set at 10m/s as the fix variable. To conduct the experiment, there are variaables that need to be consider such as:

i. DBD configuration

- Parameter of airfoil (NACA 0015)

ii. Location of DBD plasma actuator

-Leading edge

iii. Angle of incidence

-Angle of attack is set to be $0^\circ, 3^\circ, 6^\circ, 9^\circ, 12^\circ, 15^\circ, 16^\circ, 17^\circ, 18^\circ, 19^\circ, 20^\circ, 22^\circ$ and 24° .



3.3 FLOWCHART

Methodology procedure of the whole experiment in step by step as shown in flow chart (Figure 3.1) below.

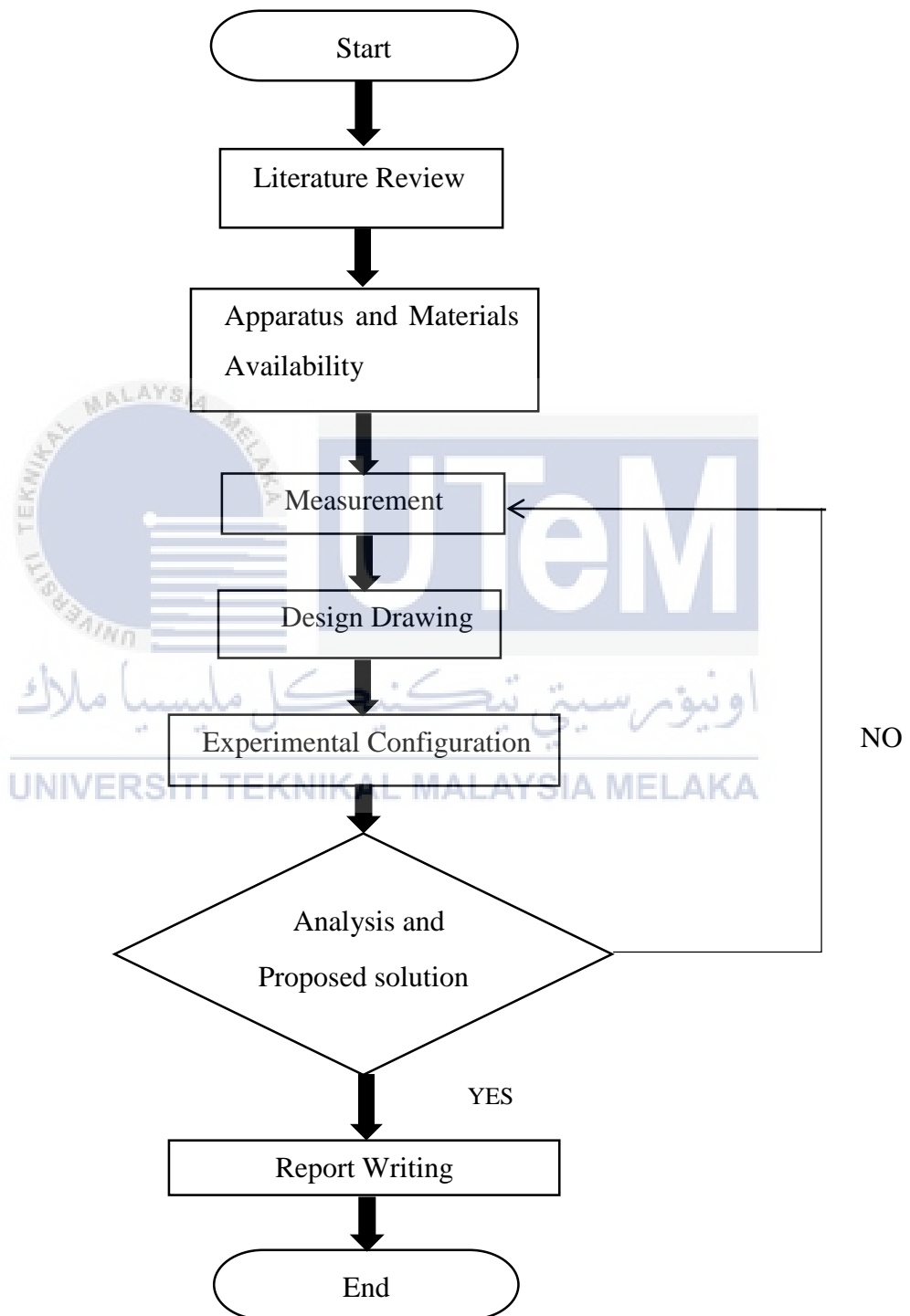


Figure 3.1: Flow Chart of the Methodology

3.4 EXPERIMENTAL EQUIPMENT

3.4.1 WIND TUNNEL

To carry out this experiment, 15m/s and 20 m/s wind velocity are used as a fixed variables. For this experiment, MP 130D Subsonic Wind Tunnel is used as shown in Figure 3.2-Figure 3.5. It is a vertical axis wind tunnel model. This model of wind tunnel used seven blade fan which is a airfoil design cast aluminium. This type of wind tunnel is suitable for NACA 0015 model airfoil as it can ensure maximum aerodynamic efficiency, less turbulence and the speed can be adjusted by using an inverter.

At contraction section, a manifold are attached by static pressure taps in order to reduce the special effects form a model and velocity of air that is shown by a manometer. The reading from the graph of manometer using air velocity is provided. In order to change the angle of incidence, holder of the model is rotated and indicated the an angular scale at the base of holder.

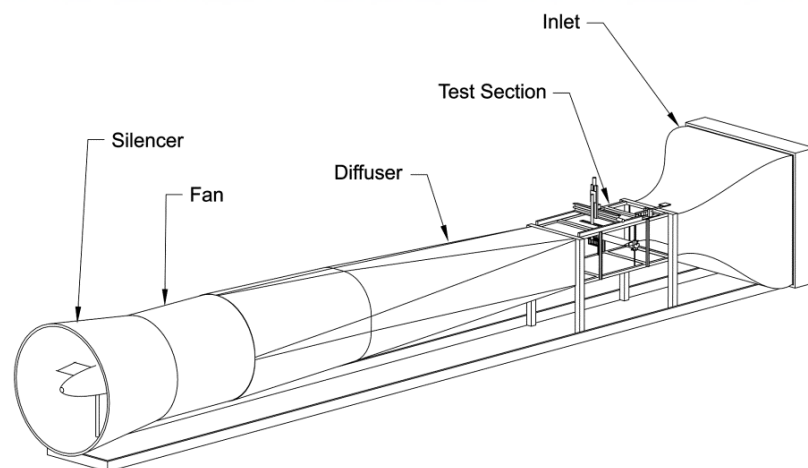


Figure 3.2: Schematic Drawing of Subsonic Wind Tunnel.

(Selig & Mcgranahan, 2004)



Figure 3.3: Front view of Subsonic Wind Tunnel.

(<https://www.linkedin.com/pulse/latest-cel-equipment-subsonic-wind>

[-tunnel-rafael-mattos-dos-santos](#))



Figure 3.4 Side View of Subsonic Wind Tunnel.

(<https://www.tequipment.com/subsonic-wind-tunnel>)

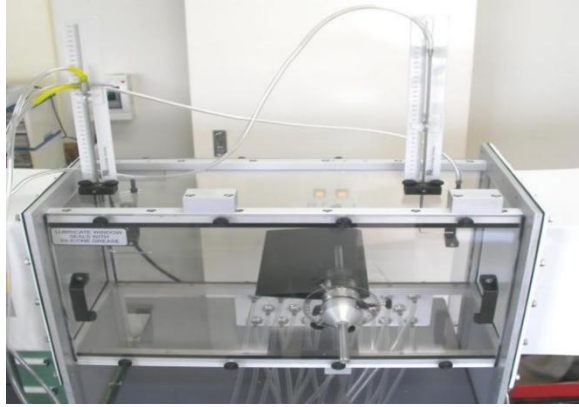


Figure 3.5: Test Section of Wind Tunnel

The wind tunnel specification is shown as below:

*Nett dimension : 3700 mm x 1065 mm x height 1900 mm

*Weight (Assembled) : 293 kg

*Test section : 300 mm x 300 mm x 450 mm long

*Air velocity : 0 to 36m/s

*Noise levels : 80 dB(A) at operators ear level

*Electrical supply : 220 V to 240 V, and 60Hz

:

3.4.2 NACA 0015 AIRFOIL

A low speed type of wind tunnel is used on the NACA 0015 airfoil model. The chord and span length of the airfoil are 10 cm and 15 cm. Thus, the aspect ratio AR for this airfoil is 1.5. This model is a symmetrical airfoil which has thickness of 15% to chord ratio. The airfoil is placed vertically inside the wind tunnel chamber. The fixed support is attached at twenty five percent from the leading edge of this model airfoil. The holder of the model or

the fixed support is used to install airfoil on the load cell. It is rotated to change the angle of incidence that test from 0 to 24 degree.

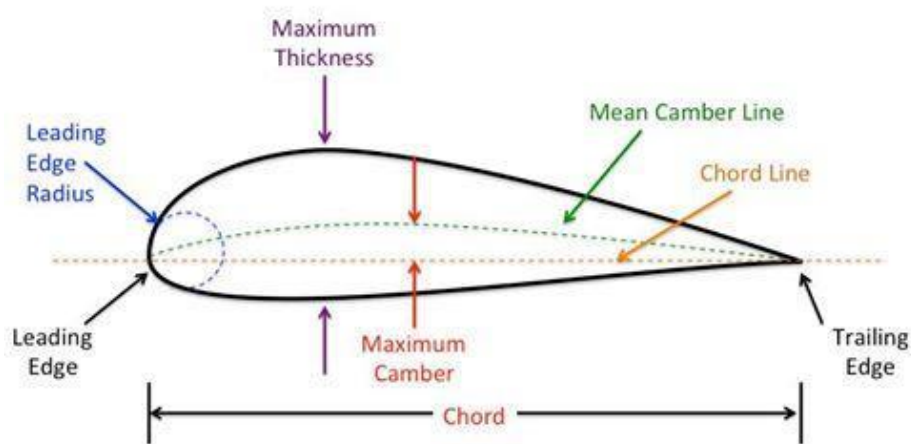


Figure 3.6: NACA 0015 with labels.

(https://www.researchgate.net/figure/292134281_fig1_Fig1-Airfoil-nomenclature-source)

3.4.3 DBD PLASMA ACTUATOR

DBD plasma actuator with the length of 0.15cm and 0.3 m in thickness is used in this experiment. This plasma actuator consists of two copper-tape electrodes, and each one of them has thickness of 50 μm and 5 mm wide. The electrodes which are exposed electrode and encapsulated electrodes) are arranged in parallel with a 1mm overlap. This plasma actuator is placed at the leading edge of the NACA 0015 airfoil. The NACA 0015 airfoil with DBD plasma actuator is tested by using wind tunnel in order to determine the drag and lift coefficient that affect the aerodynamic performances.

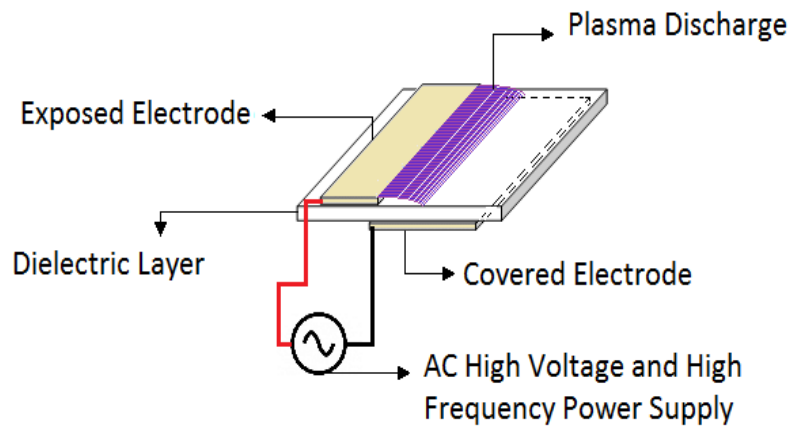


Figure 3.7: DBD plasma actuator in schematic diagram.

(https://www.researchgate.net/figure/310632302_fig1_Figure-1-Schematic-of-a-DBD-plasma-actuator)

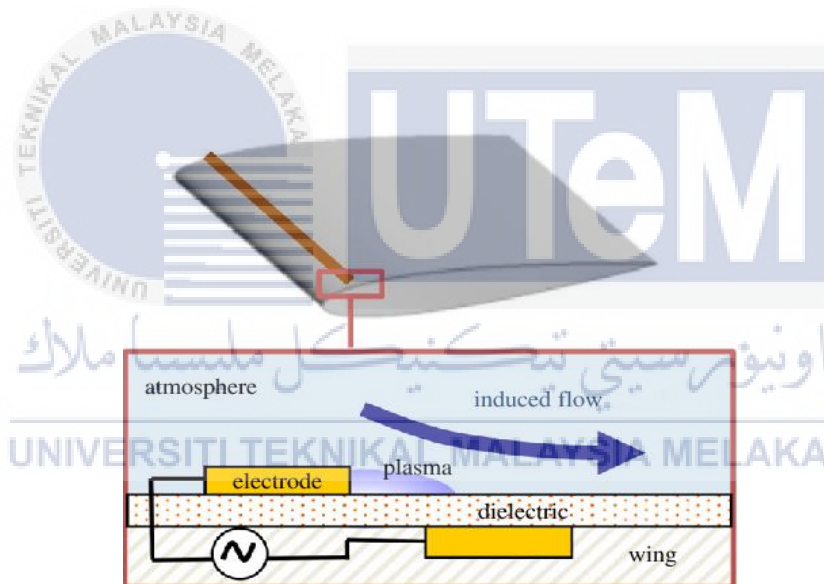


Figure 3.8: DBD plasma actuator on an airfoil. (Fujii, 2014)

3.5. DESIGN DRAWINGS

For modeling of the NACA 0015 Airfoil model, the computer aided design software used was computer aided three dimensional interactive application (CATIA). The version used to design the product for this study was CATIA V5R18. This software is developed by the French company Dassault Systems. For Mechanical Engineering, CATIA enables the creation of 3D parts, from 3D sketches, sheet metal, composites, molded, forged or tooling parts up to the definition of mechanical assemblies. For this study the product is sketched first then is transformed into 3D model using CATIA as the platform software. Once the software is opened, to start the sketching process, click on the start **Start** command at the upper right corner and then it will show a list of different processes and here click the shape

 option and then choose generative shape design. After clicking the generative shape design, a window as shown in figure 3.8 will pop up, tick only in the box for enabled hybrid design. The part name can be named here.

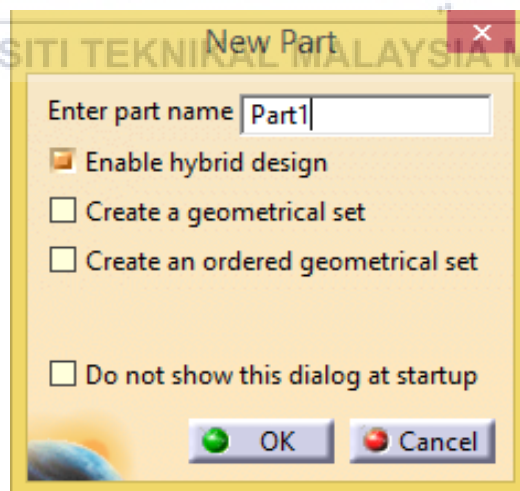


Figure 3.9: A window that appears upon clicking the part design option

After that, a new window will appear with various features on the sides to assist user during the sketching process. Next is selecting the plane to draw the sketching. There are three different options to choose from which are xy plane, yz plane and zx plane. Upon selecting the plane, next step is to insert coordinate of an airfoil into CATIA. The coordinate is obtained from airfoiltools.com. The dimension and coordinate of the airfoil used is standard for this NACA 0015 airfoil model. The coordinate was downloaded from the website. The coordinate file is opened using Microsoft Excel. Then, copy the content of GSD PointSplineLoftFromexcel file from Dassault system in the PC and paste it into coordinate file. Then, the Macros icon in the Microsoft Excel is clicked and run the main file as shown in figure 3.9(a)-(b).

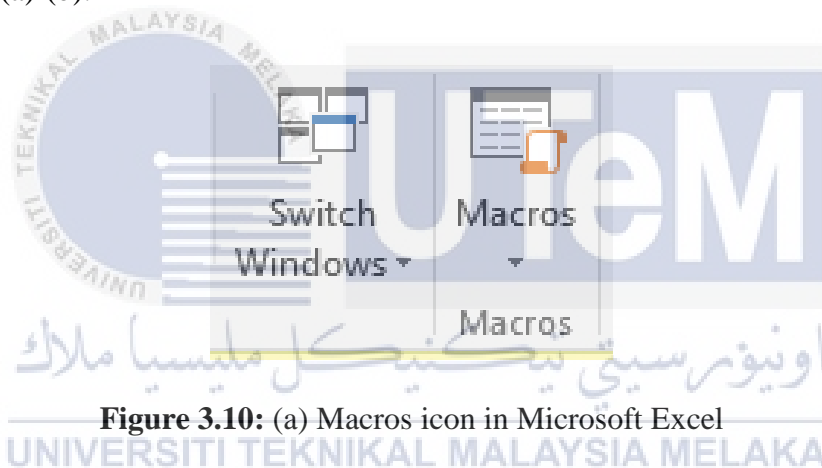


Figure 3.10: (a) Macros icon in Microsoft Excel

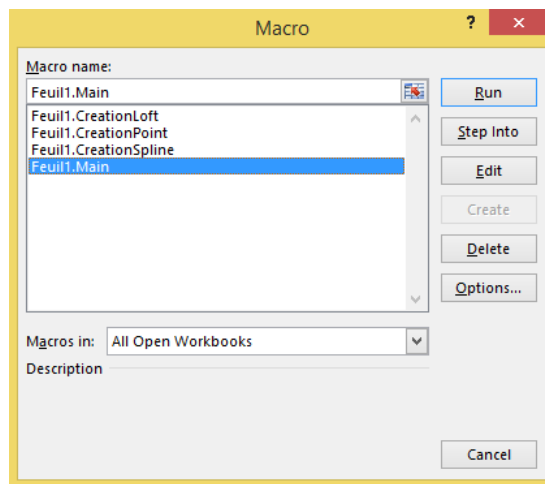
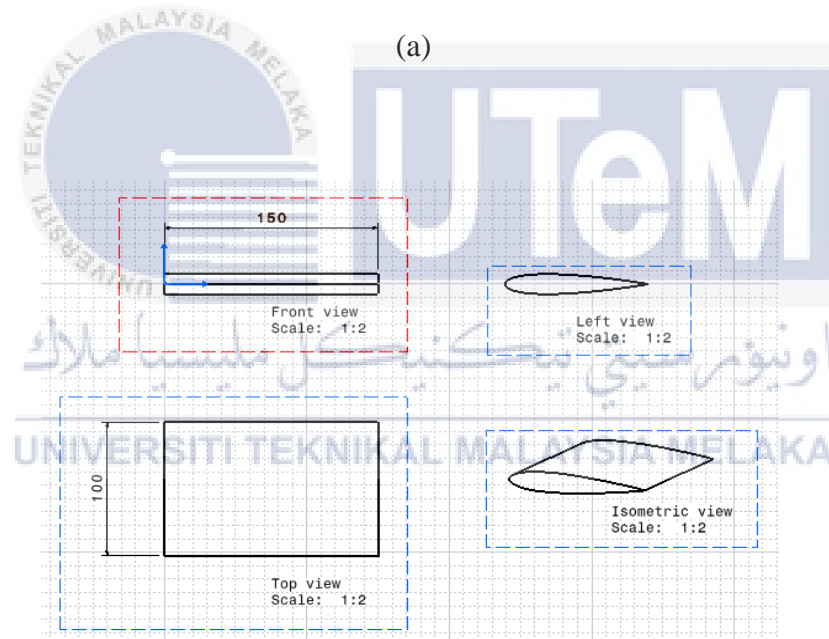
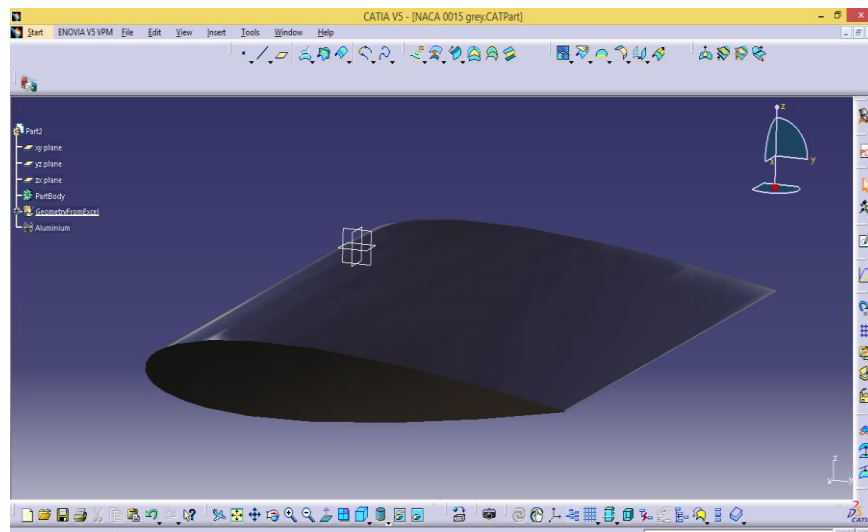


Figure 3.10: (a) Macros icon in Microsoft Excel; (b) Run the main file using Macros

3.5.1 NACA 0015 AIRFOIL DRAWING



(b)

Figure 3.11: (a) NACA 0015 airfoil model; (b) Views for each sides of Airfoil drawing

Figure 3.10 (a) shows the design of NACA 0015 Airfoil model and figure 3.10 (b) show the views for each sides of airfoil drawing. For the study, airfoil type NACA 0015 is used. The chord length of 10 cm and span length of 15 cm for this airfoil. It has a maximum thickness of fifteen percent at thirty percent of chord and has the maximum camber of zero percent at zero percent of chord. This airfoil is drawn using CATIA V5R18 software.

3.6 APPARATUS SET-UP FOR EXPERIMENTAL OF WIND TUNNEL

1. The force measurement device that support the base plat under the test section is installed by setting the threaded hole for mounting the model's holding rod in parallel vertical line of hole at the bottom of the test section.
2. Model holding rod is inserted through the hole below the test section.
3. The model of an airfoil is fixed to the top of the holding and the nut is fastened tightly.
4. The model is verified and is square with the direction of air speed and angle of attack is 0 by observing the center line of the model from the top of the test section..
5. The actuator is tested on the airfoil at the leading edge.

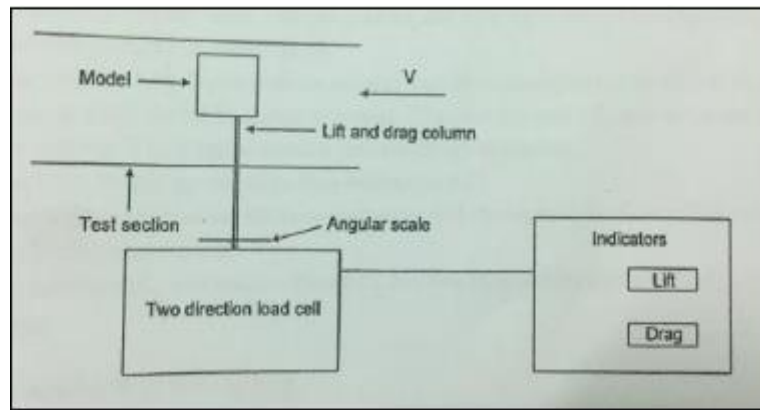


Figure 3.12: Lift and drag forces measurement against angle of incidence at different with velocity

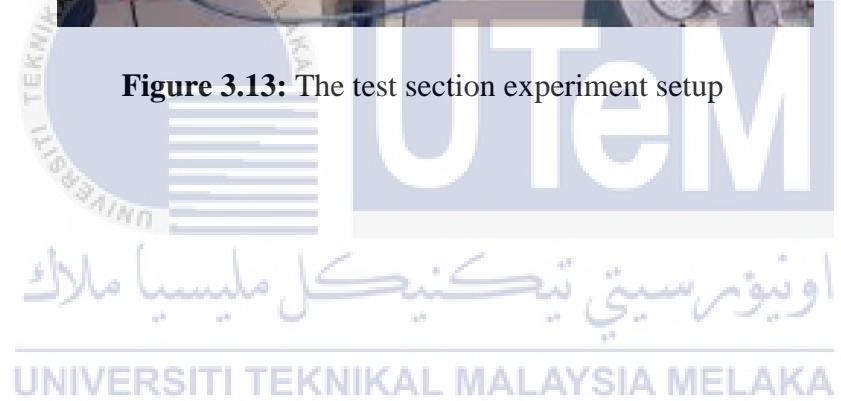
3.6.1 PROCEDURE OF EXPERIMENT

1. The drag and lift force monitor screen is linked to the force measuring device. The initial values on the data sheet is recorded if the reading on the screen is not equal to 0.
2. The fan motor is turned on and the rotation speed is altered until the required air velocity is achieved by checking from the measurement of the inclined manometer against the calibrated velocity graph.
3. The values of drag force and lift force is recorded.
4. The model holding rod is rotated with increasing angle of incidence and the value of drag and lift is recorded.
5. Repeat the step 4 by increasing the angle until the angle of incidence on the model is at 24 degree position.
6. Graphs showing the both forces comparing with the angle of attack of the testing model is plotted.

7. The lift Coefficient C_L and drag coefficient C_D per data sheet is and the plot graph of C_L and C_D and angle of attack is calculated.



Figure 3.13: The test section experiment setup



CHAPTER 4

RESULTS ANALYSIS & DISCUSSION

4.1 INTRODUCTION

In this chapter, experimenting results of C_L and C_D are presented. The obtained results are the numerical measurement of aerodynamic performance, which allows documentation of the lift and drag coefficient. The trends of the graph can be observed and relate the condition with the principal of fluid mechanics. The effects of Dielectric Barrier Discharge (DBD) plasma can be examined through the relationship between angle of attack and value of coefficient of lift, C_L and coefficient of drag, C_D .

Besides that, the position of leading edge of the NACA 0015 aerofoil are also been examined. The DBD plasma are applied on the surface of the aerofoil and tested with different angle of attack from 0° to 24° .

Additionally, data recorded will be compared and determined based on aerodynamics performance. Prediction towards the aerodynamics performance is based on the C_L and C_D obtained from the experimental data.

4.2 DRAG COEFFICIENTS

Normally, drag force, F_D indicated by;

$$F_D = \frac{1}{2}\rho v^2 C_D A - [1]$$

Which, C_D is refer to the drag coefficient, a dimensionless ratio. For the entirely occupied body condition, it can be presented by dimensional analysis and dynamic similarity

that C_D is a function of Reynold number, $N_R = \rho vd/\mu$. Next, Figure 4.1 till Figure 4.2 below show the plots of Drag Coefficient case, C_D against angle of attacks for NACA 23015 Airfoil.

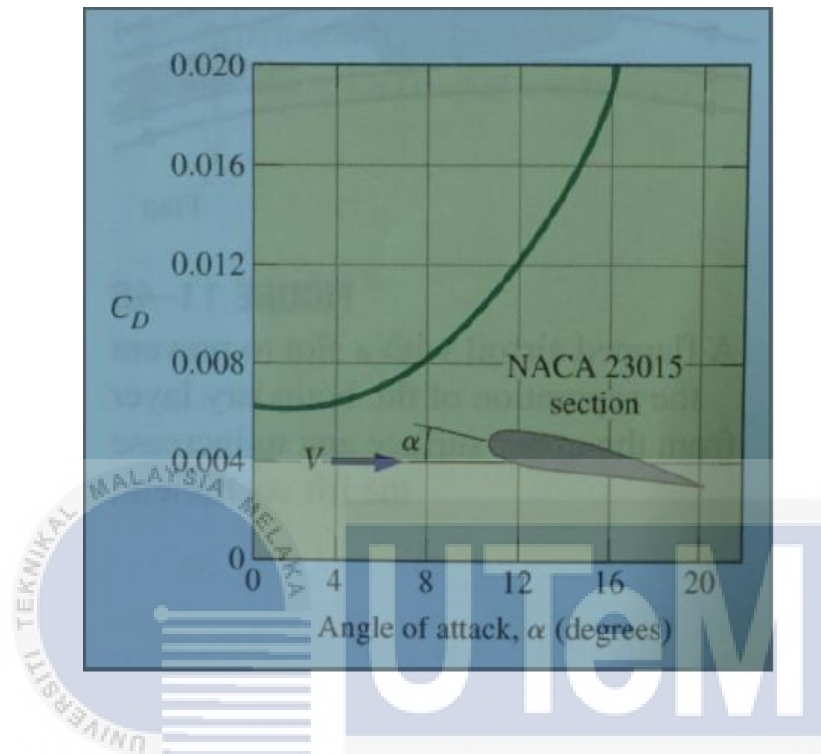


Figure 4.1: Drag Coefficient Plotted against Angle of Attack for NACA 23015 Airfoil.

(Yunus A.Cengel @ John M Cimbalà, 2014)

UNIVERSITI TEKNIKAL MALAYSIA MELAKA

4.3 LIFT DEVELOPMENT

Figure 4.2 below indicates several agreements usually applied for discussion of vanes or section of an airfoil. The symmetrical chord of length c is an uninformed line regularly recognized by designers in setting up the section. The angle θ concerning the chord and the line of uninterrupted velocity V is known as the angle of attack.

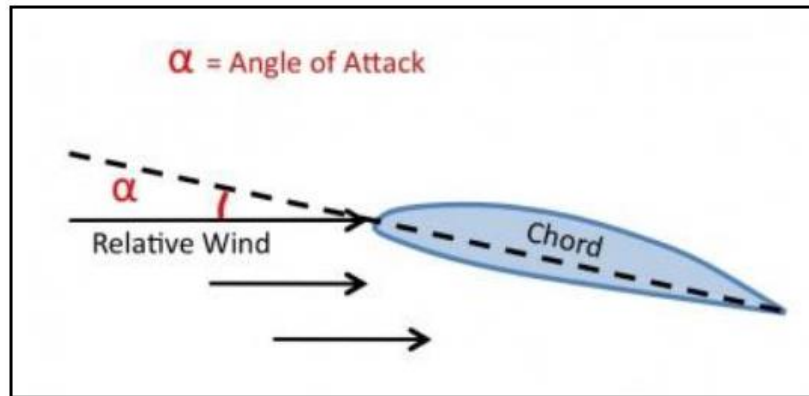


Figure 4.2: Notation of a Lifting Vane

(https://www.skybrary.aero/index.php/Angle_of_Attack)

Furthermore, Figure 4.3 next displays a diagram of the two dimensional flow through a vane segment positioned at an angle of attack perpendicularly with the fluid flow. The streamlines were similarly move apart by specific gap during the initial point of fluid flow but then it transformed after the flow passed through the section representing the velocity different by the flowing fluid. Also included is the properties on pressure distribution throughout the section.

Let

V = velocity

p_o =pressure at some distance upstream from the section

P =pressure at any point on the vane surface

The upstream velocity or dynamic pressure is indicated by the formula of $1/2\rho V^2$.

It is a usual step to define pressure distribution dimension in terms of a pressure coefficient P which is a dimensionless ratio defined as:

$$P = (p - p_o) / (1/2 \rho V^2) \quad [2]$$

The upstream pressure p_o is constant. The pressure p is calculable by conducting an experiment and could be above or lower than p_o .

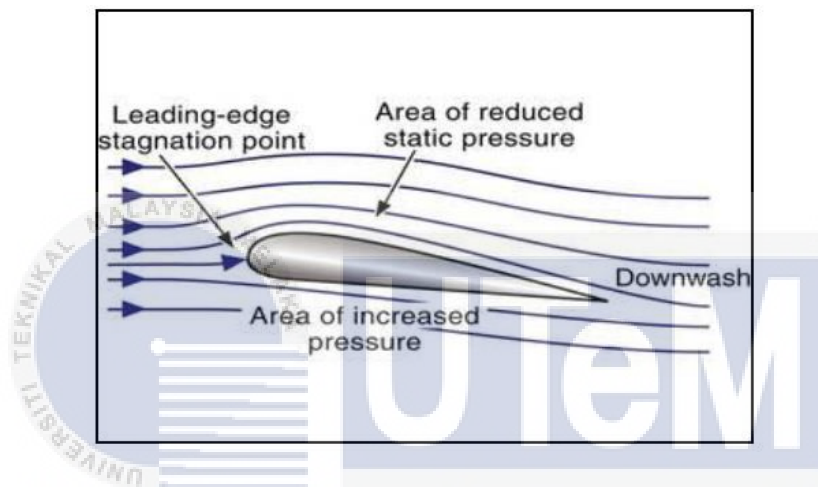


Figure 4.3: Two-dimensional Flow around a Lifting Vane

(<http://www.pilotwings.org/airfoil-pressures.html>)

Besides that, Figure 4.4 illustrated an example of pressure distribution experimental data. The pressure coefficient is plotted and gain the positive value moving downward while negative values moving upward for the change of point alongside the section surface. The net area concerning the two plotted curves, lift coefficient against chord distance in percentage of summation length is nearly proportional to the lift force due to the pressures are perpendicular to the surface and not precisely in the direction of the lift.

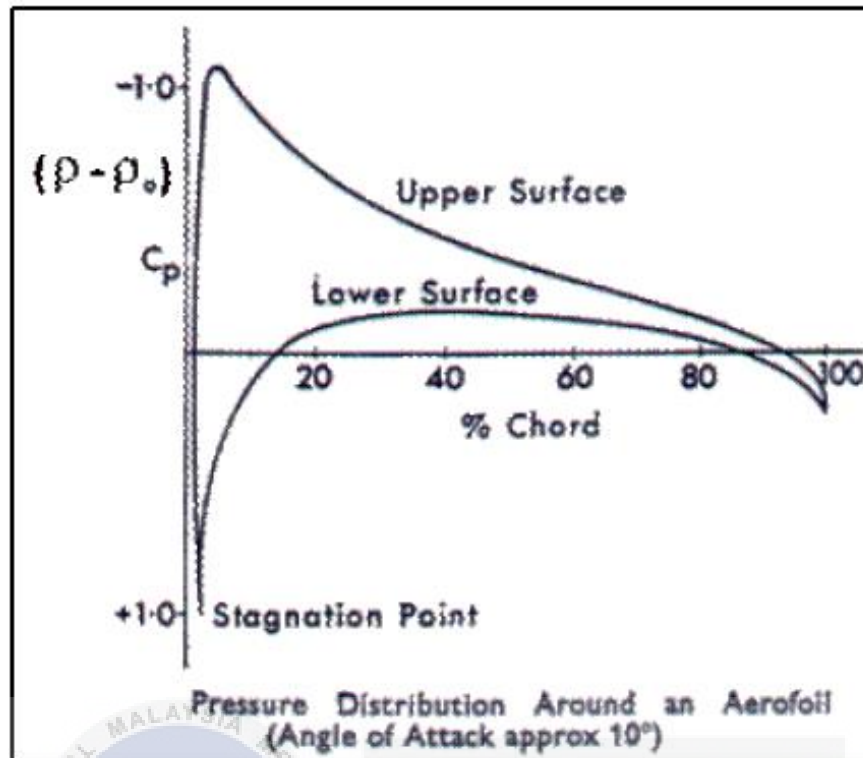


Figure 4.4: Pressure Distribution for an Airfoil

(<http://www.scrigroup.com/limba/engleza/114/Pressure-Distribution-on-an-Ae75232.php>)

4.4 LIFT COEFFICIENTS

Lift force is indicated with the following formula;

$$F_L = \frac{1}{2} \rho v^2 C_L A \quad [3]$$

Where the lift coefficient C_L is a dimensionless. The total area A is generally recorded as the estimated area.

Numerical calculation of experimental data of lift and drag coefficient for various type of airfoil sections can be obtained in numerous reports that have been distributed by NACA.

Figure 4.5 displays an example of lift and drag coefficient rises till it reaches a maximum

point then it drops as the angle of attack increases. The situation occurs is also known as stall which the condition of a lifting vane operational at an angle of attack is greater compare to the angle of attack of maximum lift. At the stall point, the working fluid split up from the vane and forms a clear eddying wake or also refer to the swirling of a fluid and create turbulent. The amount of drag coefficient will rise sharply corresponding to the stall condition is occurred.

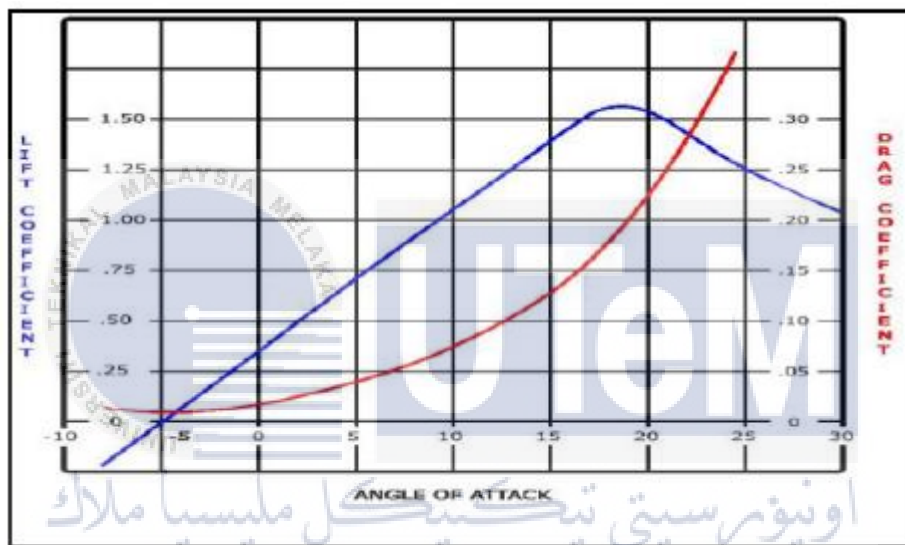


Figure 4.5: Lift and Drag Coefficients against Angle of Attack for an Airfoil

(<http://flyacro.us/spintraining.html>)

4.5 BOUNDARY LAYER

For this case of study, the stall effect is due to the transition of boundary layer occur.

Hence, it affect the aerodynamics performance of airfoil.

4.5.1 BOUNDARY LAYER

After a working fluid is passing through a flat plate, particles of air on the surface will cohere to the flat plate. Air particles which further apart from the flat plate begin to move and velocity will steadily increase with distance from the flat plate. These is when both the laminar and turbulent boundary layers occur. At the beginning, the boundary layer occurs is laminar flow with nearly linear velocity profile, causing by the viscosity of the fluid. The laminar boundary layer may possibly turn into turbulent flow when a certain distance of flow path. The equation driven for this is the Reynolds number Re is:

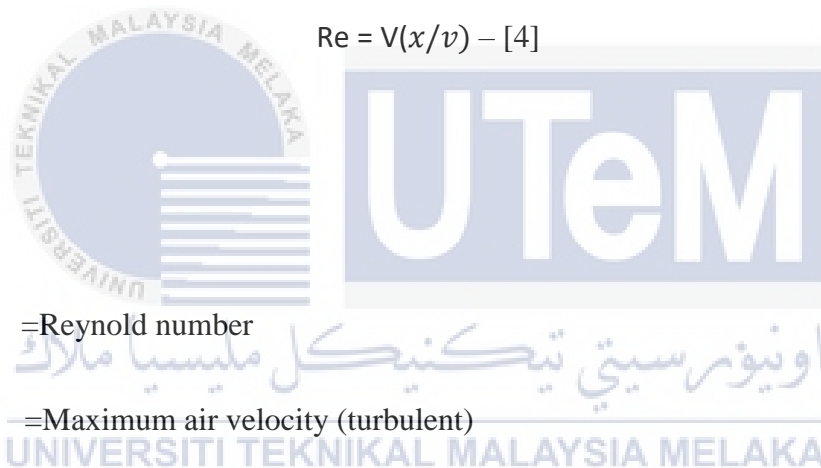
$$Re = V(x/\nu) - [4]$$

Where

Re = Reynold number

V =Maximum air velocity (turbulent)

ν =Dynamic viscosity of the fluid



Usual air velocity at boundary is shown in Figure 4.6 below.

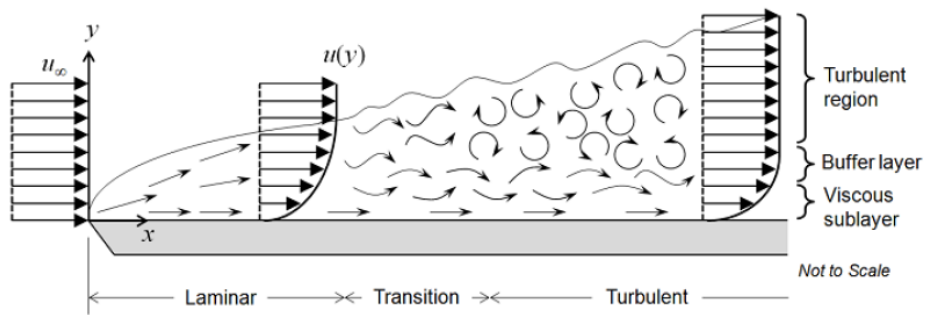


Figure 4.6: Air Velocity at Boundary. (<https://www.comsol.com/blogs/which-turbulence-model-should-choose-cfd-application/>)

4.6 EXPERIMENTAL OF AIRFOIL (BASELINE CASE) WITH SPEED OF 15 M/S SAMPLE CALCULATION

For airfoil NACA 0015 airfoil with 0 degree angle of attack (Baseline case)

Data available:

Principle Dimension:

Cross section Diameter chord = 100 mm

Width = 150 mm

$$A = 100 \times 150 = 15000 \text{ mm}^2$$

$$= 0.015 \text{ m}^2$$

Indicated Drag Force (D_o) = 0.02 N, Standard distance (X_s) = 320 mm.

Actual Drag Force (D) = D N, Actual distance (X_A) = 405 mm

$$D X_A = D_o X_s$$

$$D \times 405 = 0.02 \times 320$$

$$D = (0.02 \times 320) / 405$$

$$= 0.0158 \text{ N}$$

Indicated Lift Force (L_o) = 0.20 N, Standard distance (X_s) = 250 mm.

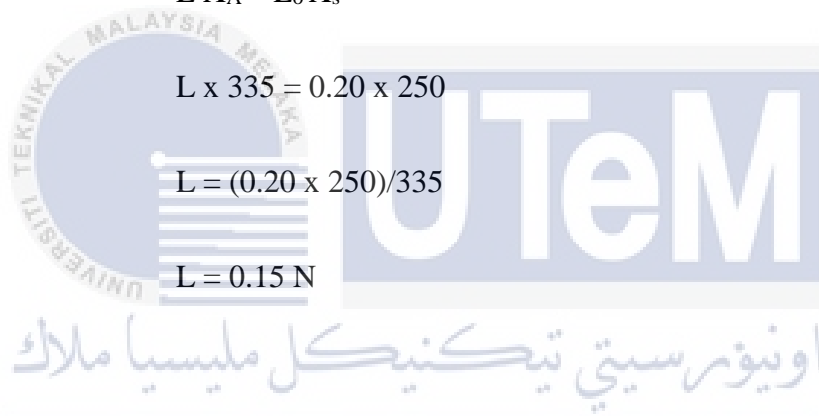
Actual Lift Force (L) = L N, Actual distance (X_A) = 335 mm.

$$L X_A = L_o X_s$$

$$L \times 335 = 0.20 \times 250$$

$$L = (0.20 \times 250) / 335$$

$$L = 0.15 \text{ N}$$



Wind Tunnel Actual Measurement;

Drag force, $D = 0.0158 \text{ N}$ Lift Force, $L = 0.15 \text{ N}$

Wind Velocity, $V = 15 \text{ m/s}$ Air Temp, $T = 35 \text{ }^\circ\text{C}$

Based from the air property table at the measured room temperature, the air properties are:

At $T = 35^\circ\text{C}$ Air Density $\rho = 1.146 \text{ kg/m}^3$

Calculation for drag and lift coefficient;

$$F_D = \frac{1}{2}\rho v^2 C_D A$$

$$F_L = \frac{1}{2}\rho v^2 C_L A$$

$$C_D = F_D / (\frac{1}{2}\rho v^2 A)$$

$$C_L = F_L / (\frac{1}{2}\rho v^2 A)$$

$$C_D = 0.0158 / (\frac{1}{2} \times 1.146 \times 15^2 \times 0.015)$$

$$C_L = 0.15 / (\frac{1}{2} \times 1.146 \times 15^2 \times 0.015)$$

$$= 0.00817$$

$$= 0.078$$



4.6.1 EXPERIMENTAL RESULTS AND ANALYSIS (BASELINE CASE)

- i. NACA 0015 Airfoil for baseline case with constant speed of 15 m/s:

Table 4.1: Experimental and Calculation Data to Determine C_L and C_D for Baseline Case.

Angle of Attack (Degree)	Initial Force (IF)		Final Force (FF)		Indicated force (IF)		Actual Force (AF)		Coefficient		Ratio
	Lift (N)	Drag (N)	Lift (N)	Drag (N)	Lift (N)	Drag (N)	Lift (N)	Drag (N)	C_L	C_D	C_L/C_D
0	0.00	-0.02	0.20	0.00	0.20	0.02	0.15	0.016	0.078	0.008	9.75
3	0.00	-0.02	0.40	0.01	0.40	0.03	0.30	0.024	0.154	0.012	12.83
6	0.00	-0.02	0.80	0.04	0.80	0.06	0.60	0.048	0.309	0.024	12.88
9	0.00	-0.02	0.96	0.07	0.96	0.09	0.72	0.071	0.370	0.037	10.00
12	0.00	-0.02	1.46	0.10	1.46	0.12	1.09	0.095	0.563	0.049	11.49
15	0.00	-0.02	2.90	0.13	2.90	0.15	2.16	0.119	1.120	0.061	18.36
16	0.00	-0.02	3.45	0.17	3.45	0.19	2.57	0.150	1.330	0.078	17.05
17	0.00	-0.02	2.36	0.20	2.36	0.22	1.76	0.174	0.911	0.090	10.12
18	0.00	-0.02	2.51	0.21	2.51	0.23	1.87	0.182	0.970	0.094	10.32
19	0.00	-0.02	2.81	0.24	2.81	0.26	2.10	0.205	1.084	0.106	10.23
20	0.00	-0.02	3.02	0.29	3.02	0.31	2.25	0.245	1.165	0.127	9.17
22	0.00	-0.02	3.14	0.31	3.14	0.33	2.34	0.261	1.212	0.135	8.98
24	0.00	-0.02	3.32	0.34	3.32	0.36	2.48	0.284	1.281	0.147	8.71

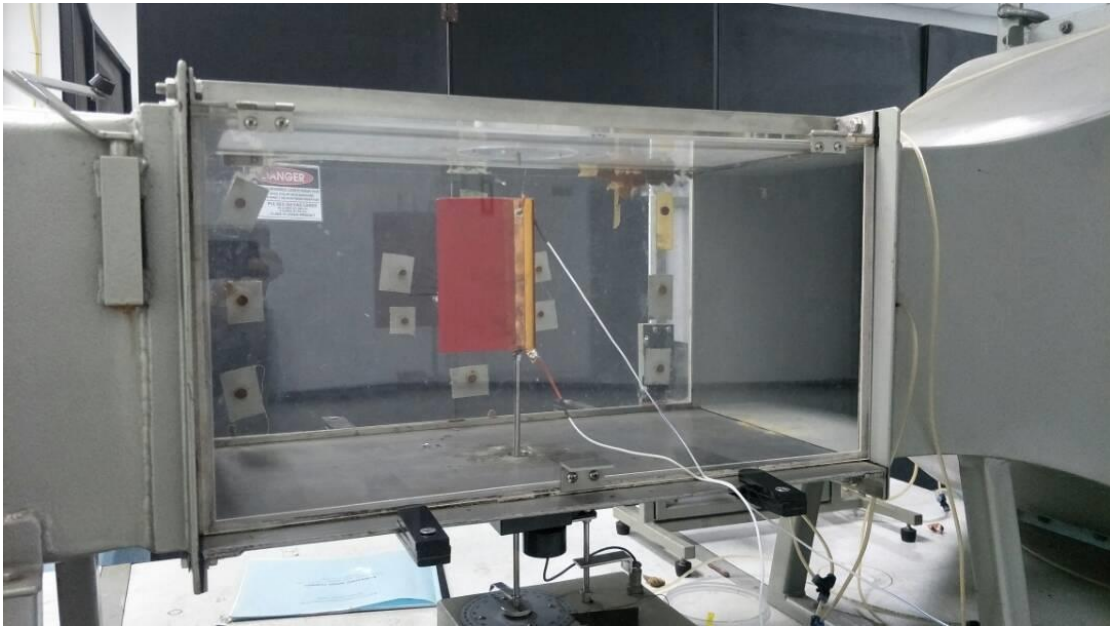


Figure 4.7: Experimental Setup for Baseline Case

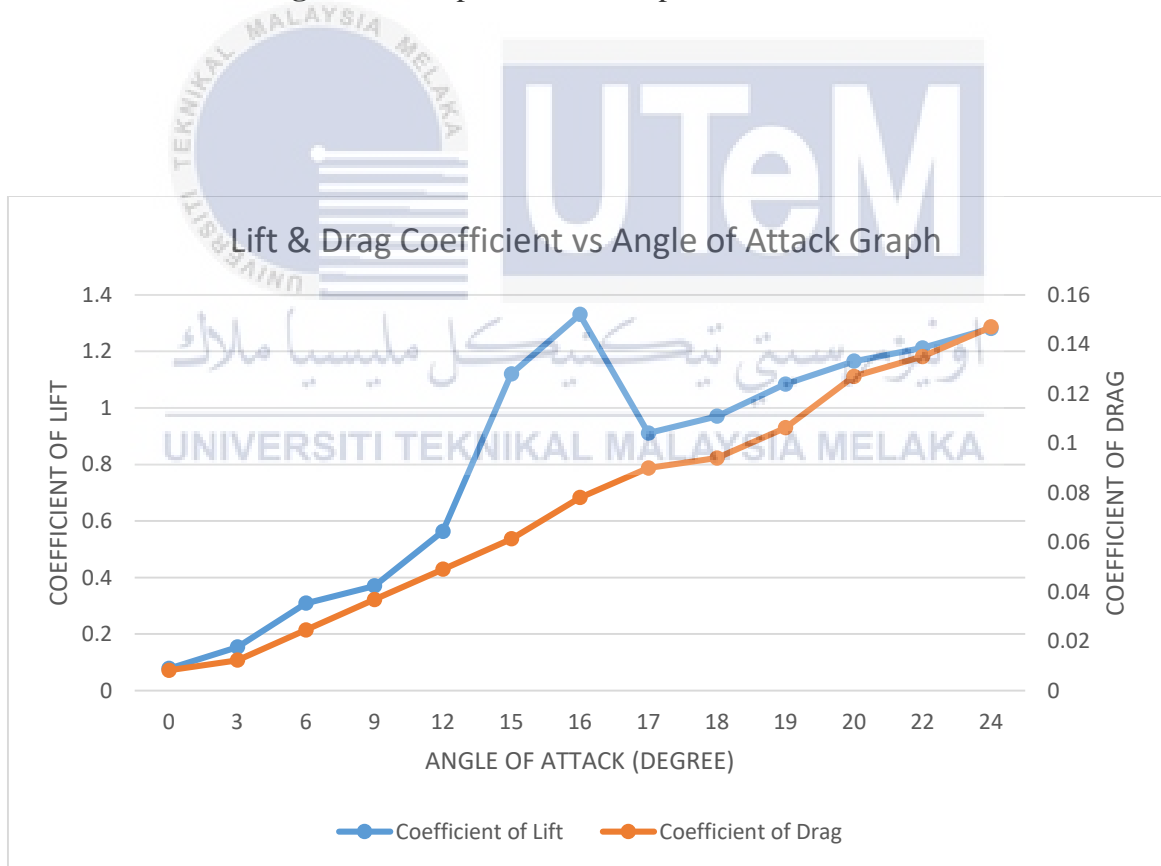


Figure 4.8: Lift and Drag Coefficient Results against Angle of Attack. (Baseline Case)

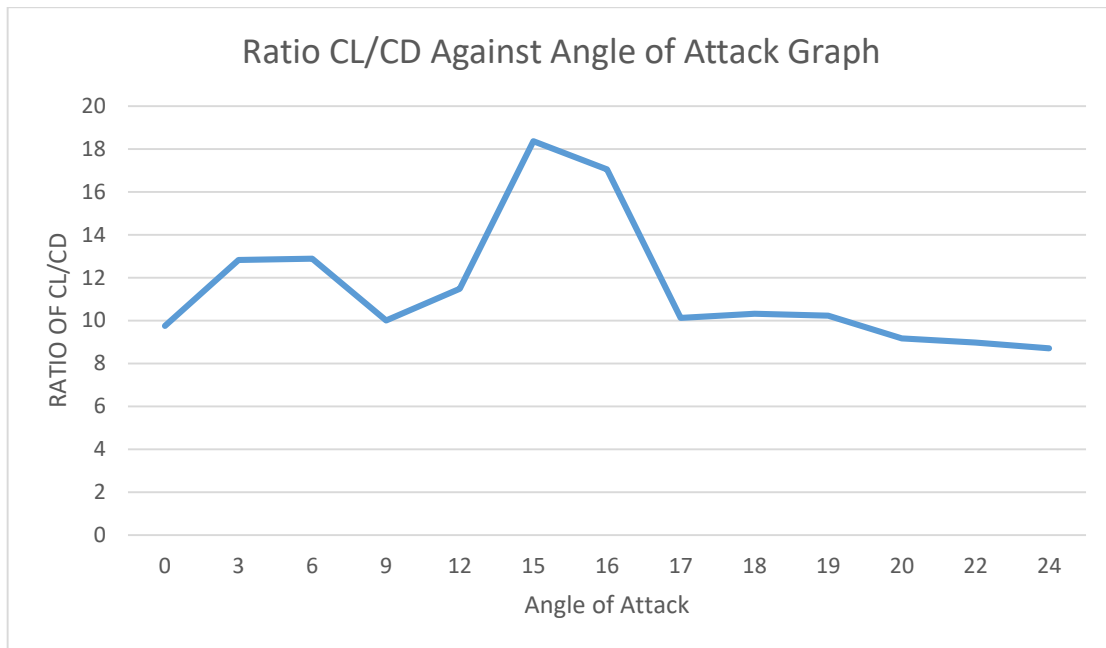


Figure 4.9: Lift and Drag Coefficient Ratio against Angle of Attack. (Baseline Case)

Table 4.1 and Figure 4.8-4.9 shows the results obtained by conducting vertical axis wind turbine experiment towards NACA 0015 for the baseline case condition (without DBD plasma actuator). The velocity of fluid is set to be constant with the value of 15 m/s and air density, $\rho = 1.146 \text{ kg/m}^3$ at room temperature of 35°C.

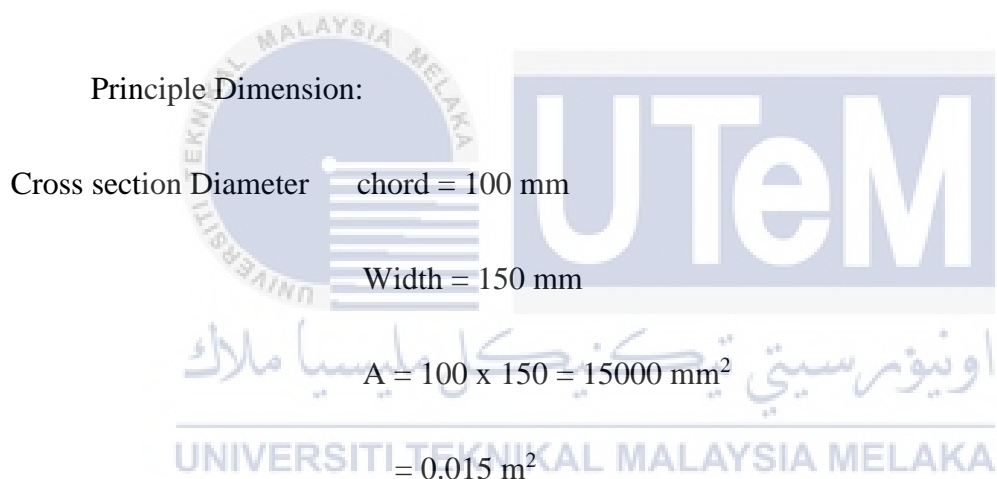
Based on the result obtained, it shows that the lift coefficient is increase steadily until it reach the critical angle of attack 16 degree and the airfoil start to undergoes stall condition at C_L value of 1.33. Then, the lift coefficient decrease drastically until 17 degree angle of attack. Then, it begins to increase steadily until it reaches the maximum angle of attack, 24° with the amount of $C_L = 1.281$. For the drag coefficient trend line, it shows the highest amount of drag coefficient value of 0.147 at 24° angle of attack. The drag coefficient increase steadily from 0° to 24°. Moreover, lift and drag coefficient ratio against angle of attack graph shows

the peak value at angle of attack, 15°. The ratio of C_L/C_D decreased gradually from 18° till it reach angle of attack, 24°.

4.7 EXPERIMENTAL OF AIRFOIL (DBD PLASMA) WITH SPEED OF 15 M/S SAMPLE CALCULATION

For airfoil NACA 0015 airfoil with 3 degree angle of attack (DBD plasma at leading edge).

Data available:



Indicated Drag Force (D_o) = 0.02 N, Standard distance (X_s) = 320 mm.

Actual Drag Force (D) = D N, Actual distance (X_A) = 405 mm

$$D X_A = D_o X_s$$

$$D \times 405 = 0.02 \times 320$$

$$D = (0.02 \times 320) / 405$$

$$= 0.0158 \text{ N}$$

Indicated Lift Force (L_o) = 0.43 N, Standard distance (X_s) = 250 mm.

Actual Lift Force (L) = L N, Actual distance (X_A) = 335 mm.

$$L X_A = L_o X_s$$

$$L \times 335 = 0.43 \times 250$$

$$L = (0.43 \times 250)/335$$

$$L = 0.321 \text{ N}$$

Wind Tunnel Actual Measurement;

Drag force, $D = 0.0158 \text{ N}$ Lift Force, $L = 0.321 \text{ N}$

Wind Velocity, $V = 15 \text{ m/s}$ Air Temp, $T = 35 \text{ }^\circ\text{C}$

Based from the air property table at the measured room temperature, the air properties are:

At $T = 35^\circ\text{C}$ Air Density $\rho = 1.146 \text{ kg/m}^3$

Calculation for drag and lift coefficient;

$$F_D = \frac{1}{2} \rho v^2 C_D A$$

$$F_L = \frac{1}{2} \rho v^2 C_L A$$

$$C_D = F_D / (\frac{1}{2} \rho v^2 A)$$

$$C_L = F_L / (\frac{1}{2} \rho v^2 A)$$

$$C_D = 0.0158 / (\frac{1}{2} \times 1.146 \times 15^2 \times 0.015)$$

$$C_L = 0.321 / (\frac{1}{2} \times 1.146 \times 15^2 \times 0.015)$$

$$= 0.00817$$

$$= 0.166$$

4.7.1 EXPERIMENTAL RESULTS AND ANALYSIS (DBD PLASMA)

- i. NACA 0015 Airfoil for DBD plasma with constant speed of 15 m/s:

Table 4.2: Experimental and Calculation Data to Determine C_L and C_D for DBD plasma Case.

Angle of Attack (Degree)	Initial Force (IF)		Final Force (FF)		Indicated force (IF)		Actual Force (AF)		Coefficient		Ratio
	Lift (N)	Drag (N)	Lift (N)	Drag (N)	Lift (N)	Drag (N)	Lift (N)	Drag (N)	C_L	C_D	C_L/C_D
0	0.00	-0.02	0.22	-0.02	0.22	0.00	0.155	0.00	0.080	0.00	0.00
3	0.00	-0.02	0.43	0.00	0.43	0.02	0.321	0.016	0.166	0.008	20.75
6	0.00	-0.02	0.82	0.02	0.82	0.04	0.612	0.032	0.316	0.016	19.75
9	0.00	-0.02	0.98	0.05	0.98	0.07	0.731	0.055	0.378	0.029	13.03
12	0.00	-0.02	1.49	0.07	1.49	0.09	1.11	0.071	0.575	0.037	15.54
15	0.00	-0.02	2.92	0.10	2.92	0.12	2.18	0.095	1.127	0.049	23.00
16	0.00	-0.02	3.48	0.14	3.48	0.16	2.60	0.126	1.343	0.065	20.66
17	0.00	-0.02	2.38	0.18	2.38	0.20	1.78	0.158	0.920	0.082	11.22
18	0.00	-0.02	2.54	0.19	2.54	0.21	1.896	0.166	0.980	0.086	11.40
19	0.00	-0.02	2.83	0.22	2.83	0.24	2.11	0.190	1.092	0.098	10.5
20	0.00	-0.02	3.04	0.28	3.04	0.30	2.27	0.237	1.173	0.123	9.54
22	0.00	-0.02	3.16	0.29	3.16	0.31	2.36	0.245	1.220	0.127	9.61
24	0.00	-0.02	3.36	0.31	3.36	0.33	2.51	0.261	1.297	0.135	9.61



Figure 4.10: Experimental Setup for DBD plasma case

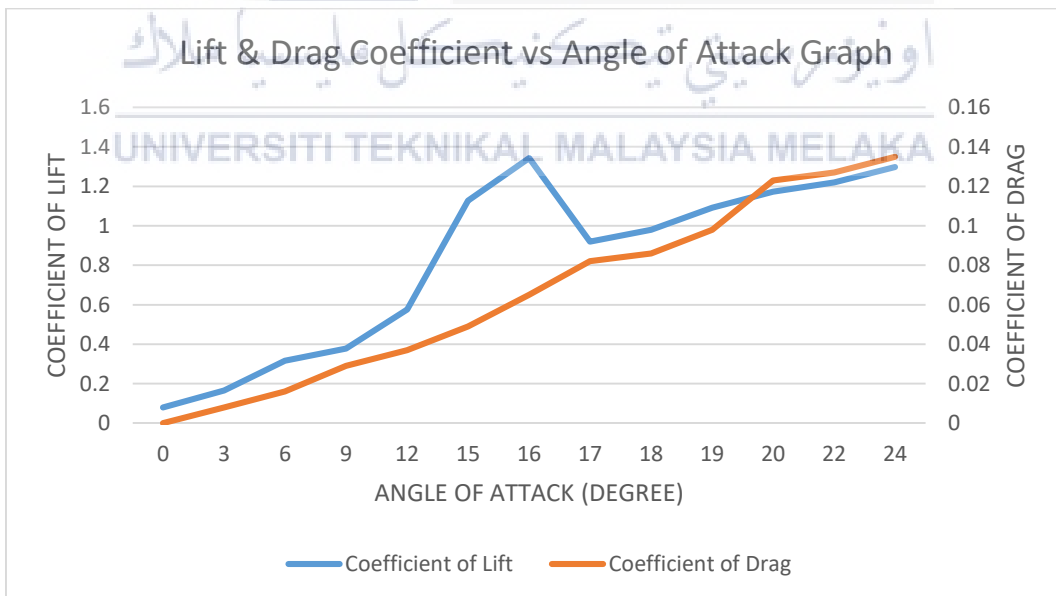


Figure 4.11: Lift and Drag Coefficient Results against Angle of Attack. (DBD plasma at leading edge) for speed of 15 m/s

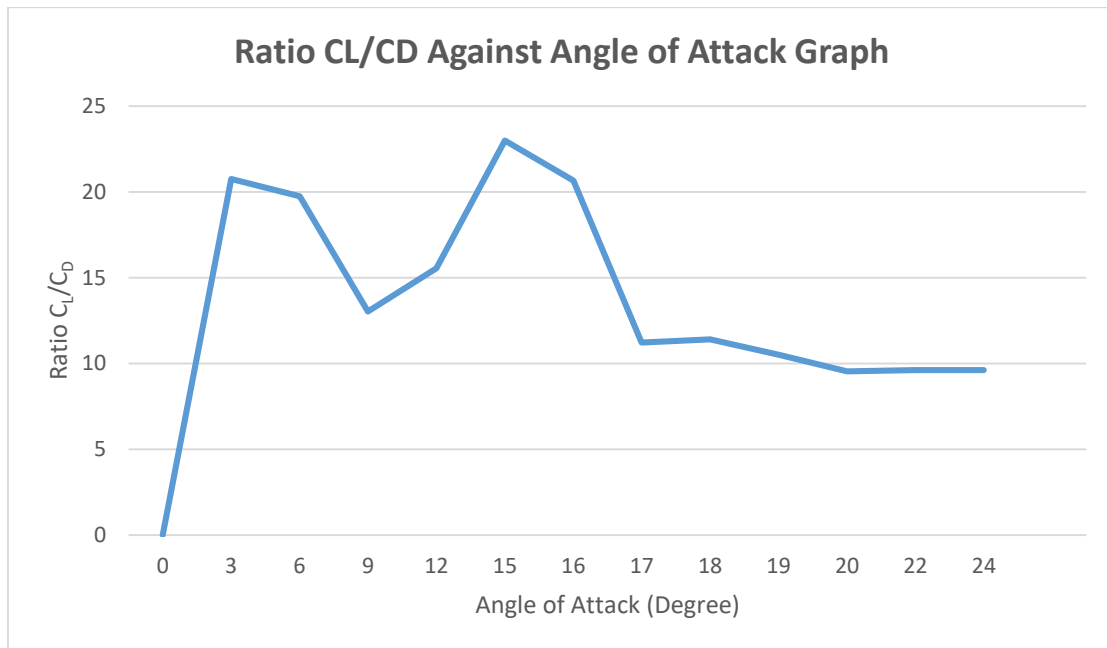


Figure 4.12: Lift and Drag Coefficient Ratio against Angle of Attack. (DBD plasma at leading edge) for speed of 15 m/s

The Dielectric Barrier Discharge (DBD) plasma is applied on the leading edge of the airfoil as shown in Figure 4.10. By referring Figure 4.11, the lift coefficient increases gradually with angle of attack α , reaches a maximum critical angle of attack about $\alpha = 16^\circ$ and then it begins to decline suddenly until it reaches angle of attack of 17° . This reduction of lift with additional increase in angle of attack is known as stall. It occurs due to the flow separation and the development of wide wake region over the top surface of the airfoil. Stall is highly undesirable since it also increases drag. Then, the lift starts to increase gradually until it reaches the maximum angle of attack applied, 24° .

By referring the C_D trend line, it shows the highest amount of drag coefficient value, 0.135 at the angle of attack, 24° . At zero angle of attack ($\alpha = 0^\circ$), the value of drag coefficient is zero. The drag coefficient increases steadily from 0° until 24° angle of attack. Moreover, lift and drag ratio against angle of attack graph shows the peak value at angle of

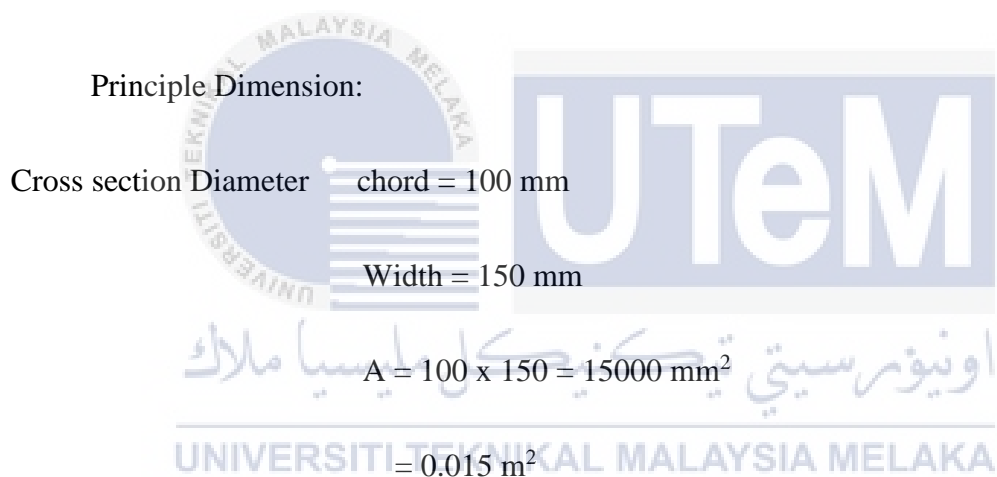
attack, 15° as shown in Figure 4.12. Next, the ratio of C_L/C_D decrease till it reach 17° .

Then, it begins to increase and decreases until it reaches at maximum angle of attack, 24° with value of 9.61.

4.8 EXPERIMENTAL OF AIRFOIL (BASELINE CASE) WITH SPEED OF 20 M/S SAMPLE CALCULATION

For airfoil NACA 0015 airfoil with 0 degree angle of attack (Baseline case)

Data available:



Indicated Drag Force (D_o) = 0.10 N, Standard distance (X_s) = 320 mm.

Actual Drag Force (D) = D N, Actual distance (X_A) = 405 mm

$$D X_A = D_o X_s$$

$$D \times 405 = 0.10 \times 320$$

$$D = (0.10 \times 320) / 405$$

$$= 0.079 \text{ N}$$

Indicated Lift Force (L_o) = 1.22 N, Standard distance (X_s) = 250 mm.

Actual Lift Force (L) = L N, Actual distance (X_A) = 335 mm.

$$L X_A = L_o X_s$$

$$L \times 335 = 1.22 \times 250$$

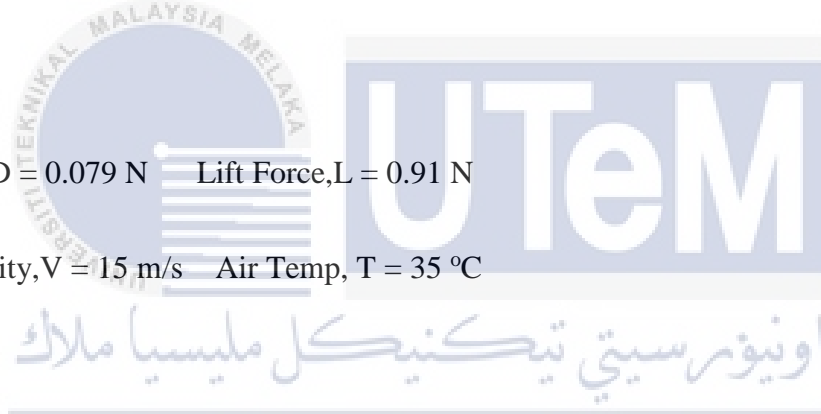
$$L = (1.22 \times 250)/335$$

$$L = 0.91 \text{ N}$$

Wind Tunnel Actual Measurement;

Drag force, $D = 0.079 \text{ N}$ Lift Force, $L = 0.91 \text{ N}$

Wind Velocity, $V = 15 \text{ m/s}$ Air Temp, $T = 35 \text{ }^\circ\text{C}$



Based from the air property table at the measured room temperature, the air properties are:

At $T = 35^\circ\text{C}$ Air Density $\rho = 1.146 \text{ kg/m}^3$

Calculation for drag and lift coefficient;

$$F_D = \frac{1}{2} \rho v^2 C_D A$$

$$F_L = \frac{1}{2} \rho v^2 C_L A$$

$$C_D = F_D / (\frac{1}{2} \rho v^2 A)$$

$$C_L = F_L / (\frac{1}{2} \rho v^2 A)$$

$$C_D = 0.079 / (\frac{1}{2} \times 1.146 \times 15^2 \times 0.015)$$

$$C_L = 0.91 / (\frac{1}{2} \times 1.146 \times 15^2 \times 0.015)$$

$$= 0.041$$

$$= 0.471$$

4.8.1 EXPERIMENTAL RESULTS AND ANALYSIS (BASELINE CASE)

- i. NACA 0015 Airfoil for baseline case with constant speed of 20 m/s:

Table 4.3: Experimental and Calculation Data to Determine C_L and C_D for Baseline Case.

Angle of Attack (Degree)	Initial Force (IF)		Final Force (FF)		Indicated force (IF)		Actual Force (AF)		Coefficient		Ratio
	Lift (N)	Drag (N)	Lift (N)	Drag (N)	Lift (N)	Drag (N)	Lift (N)	Drag (N)	C_L	C_D	
0	0.00	-0.02	1.22	0.08	1.22	0.10	0.910	0.079	0.471	0.041	11.49
3	0.00	-0.02	1.42	0.10	1.42	0.12	1.060	0.095	0.548	0.049	11.18
6	0.00	-0.02	1.63	0.13	1.63	0.15	1.216	0.119	0.629	0.061	10.31
9	0.00	-0.02	2.12	0.16	2.12	0.18	1.582	0.142	0.818	0.074	11.05
12	0.00	-0.02	3.26	0.19	3.26	0.21	2.433	0.166	1.260	0.086	14.65
15	0.00	-0.02	4.25	0.22	4.25	0.24	3.172	0.190	1.640	0.098	16.73
16	0.00	-0.02	5.61	0.27	5.61	0.29	4.187	0.229	2.165	0.118	18.35
17	0.00	-0.02	4.02	0.31	4.02	0.33	3.000	0.261	1.551	0.135	11.49
18	0.00	-0.02	4.24	0.36	4.24	0.38	3.164	0.300	1.636	0.155	10.55
19	0.00	-0.02	4.40	0.39	4.40	0.41	3.284	0.324	1.700	0.168	10.12
20	0.00	-0.02	4.82	0.42	4.82	0.44	3.600	0.348	1.860	0.180	10.33
22	0.00	-0.02	5.18	0.45	5.18	0.47	3.870	0.371	2.000	0.192	10.42
24	0.00	-0.02	5.32	0.47	5.32	0.49	3.970	0.387	2.050	0.200	10.25

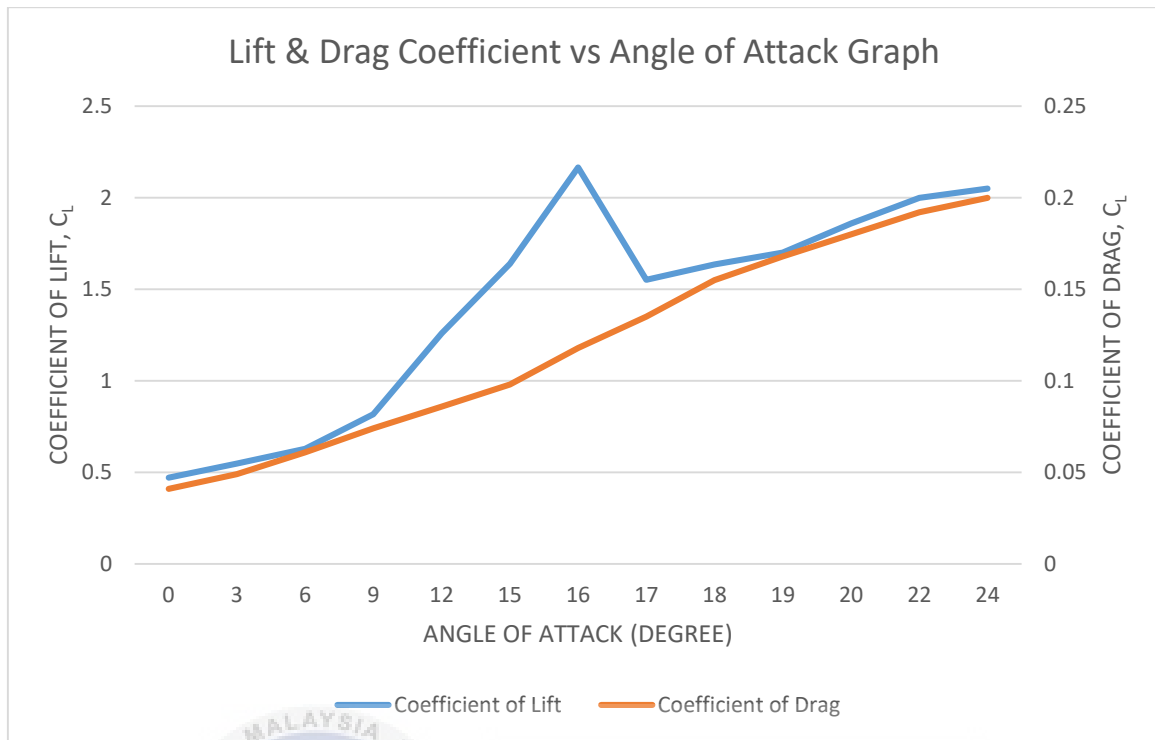


Figure 4.13: Lift and Drag Coefficient Results against Angle of Attack (Baseline Case) for speed of 20 m/s

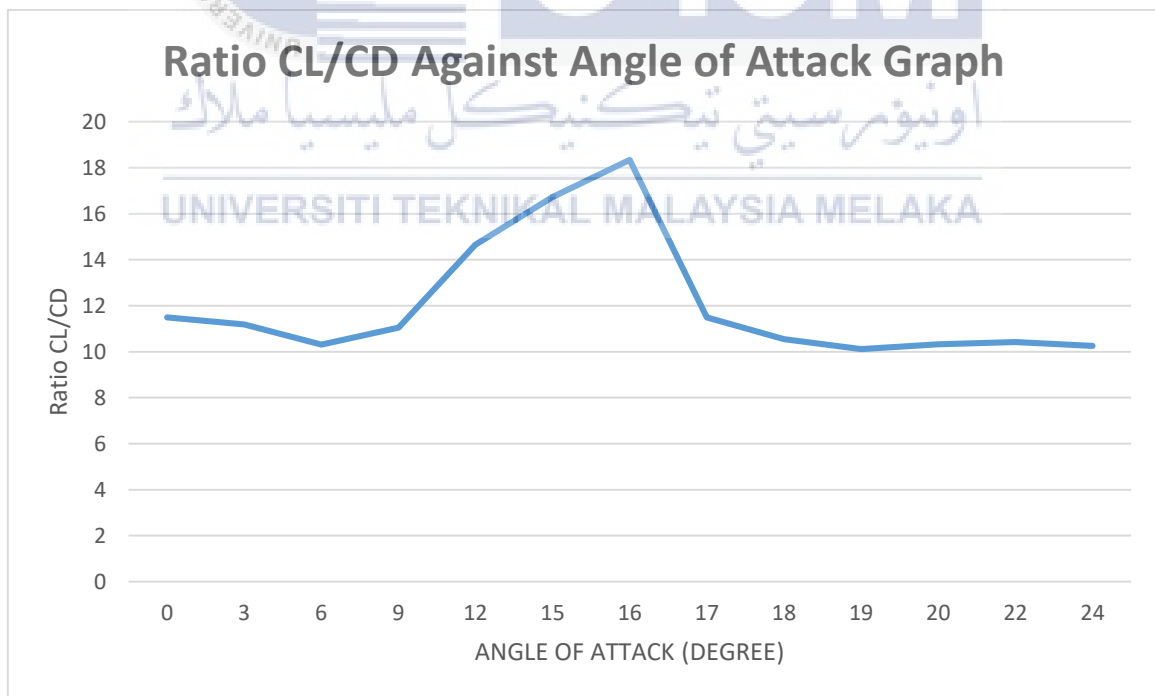


Figure 4.14: Lift and Drag Coefficient Ratio against Angle of Attack. (Baseline Case) for speed of 20 m/s

Table 4.3 and Figure 4.13 shows the results obtained by conducting vertical axis wind turbine experiment towards NACA 0015 for the baseline case condition (without DBD plasma actuator). The velocity of fluid is set to be constant with the value of 20 m/s and air density, $\rho = 1.146 \text{ kg/m}^3$ at room temperature of 35°C.

Based on the result obtained, it shows that the lift coefficient is increase steadily until it reach the critical angle of attack 16 degree and the airfoil start to undergoes stall condition at C_L value of 2.165. Then, the lift coefficient decrease drastically until 17 degree angle of attack. Then, it begins to increase steadily until it reaches the maximum angle of attack, 24° with the amount of $C_L = 2.05$. For the drag coefficient trend line, it shows the highest amount of drag coefficient value of 0.20 at 24° angle of attack. The drag coefficient increase steadily from 0° to 24°. Moreover, lift and drag coefficient ratio against angle of attack graph shows the peak value at angle of attack, 18° with value of 18.35 and lowest value at angle of attack, 19° with value of 10.12. Then, it begins to decrease gradually from angle of attack of 16° to 19°. The ratio of C_L/C_D is increase and decrease until it reaches the maximum angle of attack applied at 24°.

4.9 EXPERIMENTAL OF AIRFOIL (DBD PLASMA) WITH SPEED OF 20 M/S

SAMPLE CALCULATION

For airfoil NACA 0015 airfoil with 0 degree angle of attack (Baseline case)

Data available:

Principle Dimension:

Cross section Diameter chord = 100 mm

Width = 150 mm

$$A = 100 \times 150 = 15000 \text{ mm}^2$$

$$= 0.015 \text{ m}^2$$

Indicated Drag Force (D_o) = 0.08 N, Standard distance (X_s) = 320 mm.

Actual Drag Force (D) = D N, Actual distance (X_A) = 405 mm

$$D X_A = D_o X_s$$

$$D \times 405 = 0.08 \times 320$$

$$D = (0.08 \times 320) / 405$$

$$= 0.0632 \text{ N}$$

Indicated Lift Force (L_o) = 1.24 N, Standard distance (X_s) = 250 mm.

Actual Lift Force (L) = L N, Actual distance (X_A) = 335 mm.

$$L X_A = L_o X_s$$

$$L \times 335 = 1.24 \times 250$$

$$L = (1.22 \times 250)/335$$

$$L = 0.925 \text{ N}$$

Wind Tunnel Actual Measurement;

$$\text{Drag force, } D = 0.0632 \text{ N} \quad \text{Lift Force, } L = 0.925 \text{ N}$$

$$\text{Wind Velocity, } V = 15 \text{ m/s} \quad \text{Air Temp, } T = 35 \text{ }^\circ\text{C}$$

Based from the air property table at the measured room temperature, the air properties are:

$$\text{At } T = 35^\circ\text{C} \quad \text{Air Density } \rho = 1.146 \text{ kg/m}^3$$

Calculation for drag and lift coefficient;

$$F_D = \frac{1}{2} \rho v^2 C_D A$$

$$F_L = \frac{1}{2} \rho v^2 C_L A$$

$$C_D = F_D / (\frac{1}{2} \rho v^2 A)$$

$$C_L = F_L / (\frac{1}{2} \rho v^2 A)$$

$$C_D = 0.0632 / (\frac{1}{2} \times 1.146 \times 15^2 \times 0.015)$$

$$C_L = 0.925 / (\frac{1}{2} \times 1.146 \times 15^2 \times 0.015)$$

$$= 0.033$$

$$= 0.479$$

4.9.1 EXPERIMENTAL RESULTS AND ANALYSIS (DBD PLASMA)

- i. NACA 0015 Airfoil for DBD plasma with constant speed of 20 m/s:

Table 4.4: Experimental and Calculation Data to Determine C_L and C_D for DBD plasma

Case.

Angle of Attack (Degree)	Initial Force (IF)		Final Force (FF)		Indicated force (IF)		Actual Force (AF)		Coefficient		Ratio
	Lift (N)	Drag (N)	Lift (N)	Drag (N)	Lift (N)	Drag (N)	Lift (N)	Drag (N)	C_L	C_D	C_L/C_D
0	0.00	-0.02	1.24	0.06	1.24	0.08	0.925	0.063	0.479	0.033	14.52
3	0.00	-0.02	1.45	0.08	1.45	0.10	1.082	0.079	0.560	0.041	13.66
6	0.00	-0.02	1.66	0.11	1.66	0.13	1.240	0.103	0.641	0.053	12.09
9	0.00	-0.02	2.15	0.15	2.15	0.17	1.604	0.134	0.830	0.069	12.03
12	0.00	-0.02	3.31	0.18	3.31	0.20	2.470	0.158	1.277	0.082	15.58
15	0.00	-0.02	4.34	0.20	4.34	0.22	3.240	0.174	1.675	0.090	18.61
16	0.00	-0.02	5.64	0.23	5.64	0.25	4.210	0.198	2.176	0.102	21.33
17	0.00	-0.02	4.07	0.27	4.07	0.29	3.040	0.229	1.571	0.119	13.20
18	0.00	-0.02	4.38	0.30	4.38	0.32	3.270	0.253	1.690	0.131	12.90
19	0.00	-0.02	4.52	0.34	4.52	0.36	3.373	0.284	1.744	0.147	11.86
20	0.00	-0.02	4.89	0.37	4.89	0.39	3.650	0.308	1.891	0.159	11.89
22	0.00	-0.02	5.26	0.42	5.26	0.44	3.930	0.348	2.030	0.180	11.28
24	0.00	-0.02	5.38	0.44	5.38	0.46	4.015	0.363	2.076	0.188	11.04

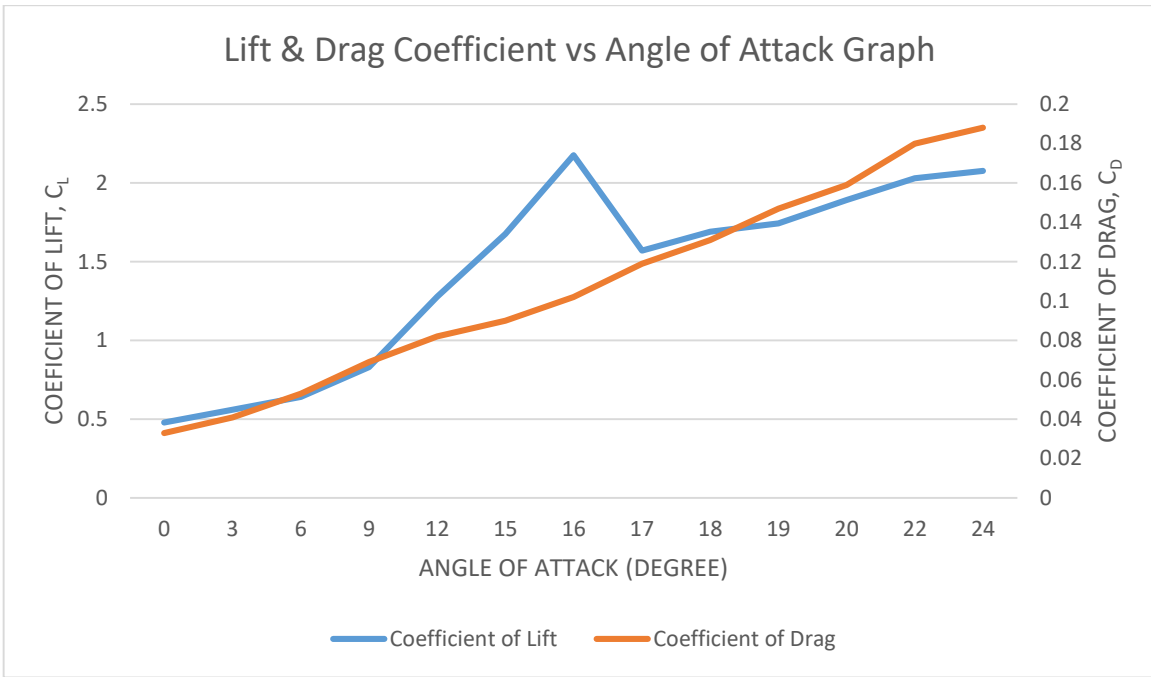


Figure 4.15: Lift and Drag Coefficient Results against Angle of Attack. (DBD plasma at leading edge) for speed of 20 m/s

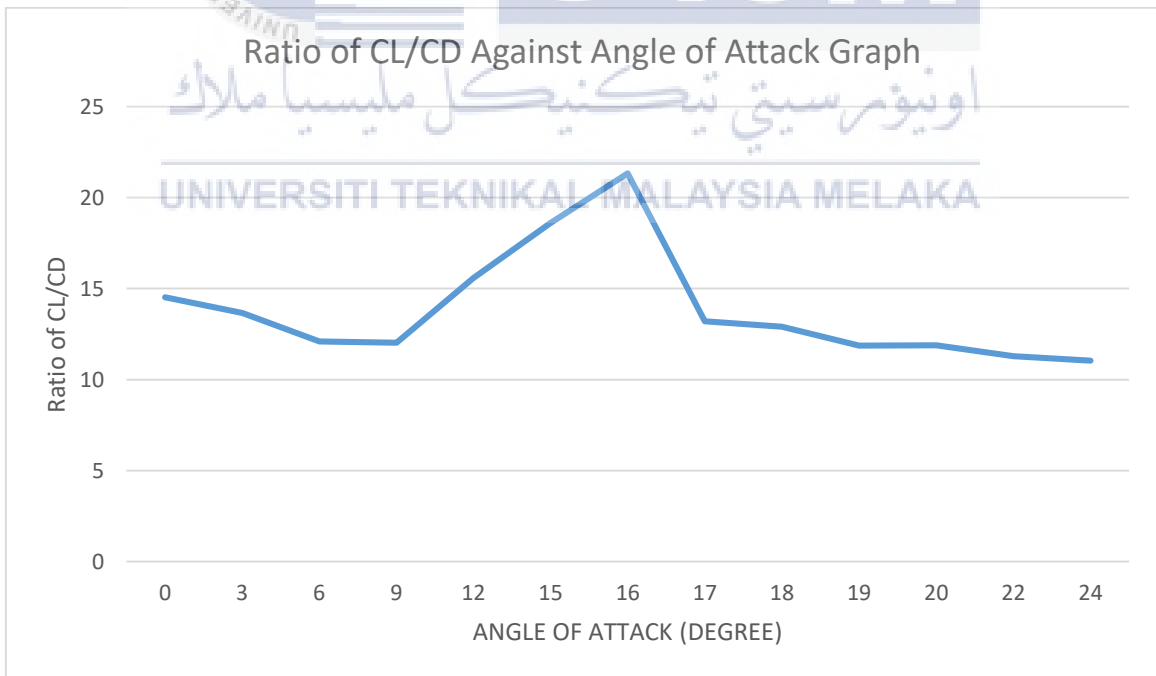


Figure 4.16: Lift and Drag Coefficient Ratio against Angle of Attack. (DBD plasma at leading edge) for speed of 20 m/s

By referring Figure 4.15, the lift coefficient increases gradually with angle of attack α , reaches a maximum critical angle of attack about $\alpha = 16^\circ$ and then it begins to decline suddenly until it reaches angle of attack of 17° . This reduction of lift with additional increase in angle of attack is known as stall. It occurs due to the flow separation and the development of wide wake region over the top surface of the airfoil. Stall is highly undesirable since it also increases drag. Then, the lift starts to increase gradually until it reaches the maximum angle of attack applied, 24° .

By referring the C_D trend line, it shows the highest amount of drag coefficient value, 0.188 at the angle of attack, 24° . At zero angle of attack ($\alpha = 0^\circ$), the value of drag coefficient is 0.033. The drag coefficient increase steadily from 0° until 24° angle of attack. Besides that, C_L/C_D ratio against angle of attack graph shows a fluctuating trend with the highest peak value of 21.33 at angle of attack, 16° as shown in Figure 4.16. Next, the ratio of C_L/C_D decrease till it reaches 19° . Then, it begins to increase and decreases until it reaches at maximum angle of attack, 24° with value of 11.04.

The highest peak value of C_L/C_D indicates the highest aerodynamic performance value compare to baseline case for speed of 20 m/s. As mentioned by earlier study, the function of Dielectric Barrier Discharge (DBD) plasma is to delay the flow separation occurs towards the airfoil. Hence, the amount of velocity or angle of attack must be increases to determine the maximum angle of attack which stalls occur for specific case.

CHAPTER 5

CONCLUSION AND RECOMMENDATION

5.1 CONCLUSION

According to the experimental result and analysis, it can be said that the application of Dielectric Barrier Discharge (DBD) plasma actuator could improve the aerodynamics performance for aerofoil. Based on the results comparison between baseline and actuation case, it shows that the airfoil with applied DBD plasma actuator shown the positive impact in aerodynamic performance. For the baseline case with speed of 15 m/s, the highest value of lift coefficient, C_L is 1.330 at 16° angle of attack. For this case, the flow separation is larger and it occur at mid stage for angle of attack. The working fluid flow started to separate from the surface of the airfoil and the streamline transform from laminar to turbulent flow. This condition produce low aerodynamics performance.

For the actuation case with speed of 15 m/s, the highest value of lift coefficient, C_L is 1.343 at 16° angle of attack. It shows slightly increase in coefficient of lift compared to the baseline case for same speed used. It is because the flow separation that occur on the airfoil is quite small compared to the baseline case. This DBD plasma actuator helps in delayed the flow separation occurs along the airfoil and maintained the boundary layer. It maintained the laminar flow attached with the upper surface of the aerofoil and produce lower drag force. Next, for the baseline case with speed of 20 m/s, the highest value of lift coefficient is 2.165 at 16° angle of attack while for the actuation case with the same speed, the highest value of lift coefficient, C_L is 2.176. From the experiment results, it also shows that the lift coefficient is increases when applied DBD plasma actuator with speed of 20 m/s. It is also due to the flow separation occur on the surface of an airfoil which is quite smaller when the DBD

plasma actuator is switched on (actuation case) compared with the baseline case when DBD plasma actuator is switched off.

For the normal baseline case, as the angle of attack of NACA 0015 Airfoil increases, separation of the airflow from the upper surface of the airfoil turn out to be extra definite causing to a decrease in the amount of rise of the lift coefficient and produce higher drag coefficient. When the lift coefficient value start to drop at the critical angle, stall occurs and lower the aerodynamics performance of the airfoil.

As a conclusion, the experimental study on the effect of DBD plasma actuator to aerodynamics performance had been obtained. The amount of lift coefficient, C_L and drag coefficient, C_D for baseline and actuation case have been compared and overly shows a positive impact of DBD plasma actuator. However, improvements must be make in the future research to make an adjustment toward the manipulated variables for positive results of responding variables. Overall for this project studies, it has achieved the objective to investigate the effect of Dielectric Barrier Discharge (DBD) plasma actuator on the leading edge of airfoil and compare the aerofoil aerodynamic performance between base case and actuation case.

5.2 RECOMMENDATION

Based on the previous chapter, the properties of Dielectric Barrier Discharge (DBD) plasma actuator that applied on the NACA 0015 Airfoil were investigated in a vertical axis wind turbine. The experimental study is focusing on the justification common aerodynamics performance influenced by DBD plasma actuator and the experiment aims to investigate the effect of Dielectric Barrier Discharge (DBD) plasma actuator on the leading edge of airfoil and compare the airfoil aerodynamic performance between base case and actuation case. The coefficient of Drag and Lift is measured for both base line and actuation cases besides obtains aerodynamic performance for NACA 0015 Airfoil.

The data recorded shows that the aerodynamic performance of actuation case be able to develop by proper arrangement of DBD plasma actuator on the airfoil. Besides, the amount of air velocity supplied is low with the amount of air velocity supplied are low with the amount of 15 m/s and 20 m/s due to the capacity of wind tunnel. The wind tunnel used can only supply till 30 m/s air velocity. Although it can supply air velocity till 30 m/s, there is a problem with the power supply. In order to prevent any electrical circuit breakdown, the speed control module reading must be increase by five units per session until it reach the demanding velocity and required a lot of time to wait for session to run. Besides that, airfoils generally function at small angle of attack, lift performance of airfoil at that settings had better be conserved after overwhelming flow separation at large angles of attacks. The incorrect arrangement of DBD plasma actuator applied on the airfoil could reduce the power supply of wind tunnel at certain operational cases.

Moreover, in order to obtain more appropriate and reliable outcomes, the experimental results must be compared with CFD result. It is because, human are tend to make errors and mistakes during conducting an experiment. There are few example of errors that can be made such as systematic errors, random errors and parallex errors. Hence, by the aid of CFD may

help in supply additional data to compare between mathematical and analytical approach. Furthermore, prototype and model comparison must be made. By conducting this comparison, the actual performance and efficiency of airfoil can be obtained and relate with the real life situation. Besides, the experiment may also be test in co-rotating fluid flow generated by DBD plasma actuator to determine which rotating flow produce better lift and drag coefficient. The implementation of Vortex generator on the surface of airfoil can also apply to obtain extra results relate with the aerodynamic performance efficiency. Those aspects must be considered for future work.



REFERENCES

Dunbar, B. (2015, May 12). What Is Aerodynamics? Retrieved October 26, 2017, from <https://www.nasa.gov/audience/forstudents/k-4/stories/nasa-knows/what-is-aerodynamics-k4.html>.

Erfani, R., Zare-Behtash, H., Hale, C., & Kontis, K. (2015). Development of DBD plasma actuators: The double encapsulated electrode. *Acta Astronautica*, 109, 132-143. doi:10.1016/j.actaastro.2014.12.016.

The Editors of Encyclopædia Britannica. (2017, April 26). Wind tunnel. Retrieved October 26, 2017, from <https://www.britannica.com/technology/wind-tunnel>.

Chapter 02: Aerodynamics of Flight - faa.gov. (n.d.). Retrieved October 26, 2017, from <https://www.bing.com/cr?IG=F5D4EBF37E9E4D52913B8B77CD737000&CID>

Aircraft Stalling. (n.d.). Retrieved October 26, 2017, from http://www.aviationsafetymagazine.com/issues/36_10/features/Aircraft-Stalling-3-Basic-Kinds_11245-1.html.

Post, M., Greenwade, S., Yan, M., Corke, T., & Patel, M. (2007). Effects of an Aerodynamic Plasma Actuator on a HSNLF Airfoil. 45th AIAA Aerospace Sciences Meeting and Exhibit. doi:10.2514/6.2007-638.

(n.d.). Lift Augmentation Devices, II. Retrieved October 27, 2017, from <https://www.experimentalaircraft.info/flight-planning/aircraft-lift-augmentation-devices-1.php>.

Bouremel, Y., Li, J., Zhao, Z., & Debiassi, M. (2013). Effects of AC Dielectric Barrier Discharge Plasma Actuator Location on Flow Separation and Airfoil Performance. *Procedia Engineering*, 67, 270-278. doi:10.1016/j.proeng.2013.12.026.

Benard, N., Jolibois, J., & Moreau, E. (2009). Lift and drag performances of an axisymmetric airfoil controlled by plasma actuator. *Journal of Electrostatics*, 67(2-3), 133-139. doi:10.1016/j.elstat.2009.01.008.

Wang, J., Choi, K., Feng, L., Jukes, T. N., & Whalley, R. D. (2013). Recent developments in DBD plasma flow control. *Progress in Aerospace Sciences*, 62, 52-78. doi:10.1016/j.paerosci.2013.05.003.

Boundary Layer Separation and Pressure Drag. (2017, November 11). Retrieved December 13, 2017, from <http://aerospaceengineeringblog.com/boundary-layer-separation-and-pressure-drag/>.

Chaudhry, I. A., Sultan, T., Siddiqui, F. A., Farhan, M., & Asim, M. (2017). The flow separation delay in the boundary layer by induced vortices. Retrieved December 13, 2017, from <https://www.ncbi.nlm.nih.gov/pmc/articles/PMC5408059/>.

Rubel, R. I., Uddin, M. K., Islam, M. Z., & Rokunuzzaman, M. (2016). Comparison of Aerodynamics Characteristics of NACA 0015 & NACA 4415. doi:10.20944/preprints201610.0095.v1.

Selig, M. S., & Mcgranahan, B. D. (2004). Wind Tunnel Aerodynamic Tests of Six Airfoils for Use on Small Wind Turbines. *Journal of Solar Energy Engineering*, 126(4), 986. doi:10.1115/1.1793208.

Fujii, K. (2014). High-performance computing-based exploration of flow control with micro devices. *Philosophical Transactions of the Royal Society A: Mathematical, Physical and Engineering Sciences*, 372(2022), 20130326-20130326. doi:10.1098/rsta.2013.0326.



APPENDIX A: Flow Chart

